JEM Journal of Experimental Medicine

ARTICLE

Monocytic MDSCs homing to thymus contribute to age-related CD8⁺ T cell tolerance of HBV

Zhong Fang[1,2], Yi Zhang[3], Zhaoqin Zhu[3], Cong Wang[1,3], Yao Hu[4], Xiuhua Peng[3], Dandan Zhang[3], Jun Zhao[3], Bisheng Shi[1,3], Zhongliang Shen[1], Min Wu[3], Chunhua Xu[3], Jieliang Chen[1], Xiaohui Zhou[3], Youhua Xie[1], Hui Yu[4], Xiaonan Zhang[3], Jianhua Li[1], Yunwen Hu[3], Maya Kozlowski[1,3], Antonio Bertoletti[5], and Zhenghong Yuan[1,3,6]

Hepatitis B virus exposure in children usually develops into chronic hepatitis B (CHB). Although hepatitis B surface antigen (HBsAg)–specific CD8⁺ T cells contribute to resolve HBV infection, they are preferentially undetected in CHB patients. Moreover, the mechanism for this rarely detected HBsAg-specific CD8⁺ T cells remains unexplored. We herein found that the frequency of HBsAg-specific CD8⁺ T cells was inversely correlated with expansion of monocytic myeloid-derived suppressor cells (mMDSCs) in young rather than in adult CHB patients, and CCR9 was upregulated by HBsAg on mMDSCs via activation of ERK1/2 and IL-6. Sequentially, the interaction between CCL25 and CCR9 mediated thymic homing of mMDSCs, which caused the cross-presentation, transferring of peripheral HBsAg into the thymic medulla, and then promoted death of HBsAg-specific CD8⁺ thymocytes. In mice, adoptive transfer of mMDSCs selectively obliterated HBsAg-specific CD8⁺ T cells and facilitated persistence of HBV in a CCR9-dependent manner. Taken together, our results uncovered a novel mechanism for establishing specific CD8⁺ tolerance to HBsAg in chronic HBV infection.

Introduction

An estimated 257 million people are living with chronic hepatitis B (CHB) virus (HBV) infection globally, which is one of the most important causative factors in the development of hepatocellular carcinoma. When more than 95% of HBV exposure is self-limiting in adults, there is a high rate of chronicity in infants and children (Liaw and Chu, 2009; Ott et al., 2012). Clearance of hepatitis B surface antigen (HBsAg) indicating functional cure is hardly achieved in patients who are exposed to HBV when they are young (Boonstra et al., 2008). Recent studies showed that CD8⁺ T cells targeting different HBV proteins, such as polymerase and HBcAg, have different features (Bertoletti and Kennedy, 2019; Hoogeveen et al., 2019; Schuch et al., 2019). Particularly, HBsAg-specific CD8⁺ T cells are rarely detectable in CHB patients (Hoogeveen et al., 2019; Rivino et al., 2018) but easily demonstrated in acute and resolving HBV infection (Thimme et al., 2003; Yang et al., 2002), These rarely detected HBsAg-specific CD8⁺ T cells in CHB patients should be the important reason for hard achievement of HBV functional cure. Nevertheless, mechanisms underlying these rarely detected HBsAg-specific CD8⁺ T cells in CHB patients remain unexplored yet.

Myeloid-derived suppressor cells (MDSCs) possess strong immunosuppressive activities to antigen-specific CD8⁺ T cells (Kusmartsev et al., 2004; Nagaraj et al., 2010; Solito et al., 2011). Previously, we reported that substantial HBsAg promotes polarization of monocytic MDSCs (mMDSCs) from monocytes in CHB (Fang et al., 2015). We herein collected blood samples from CHB patients of ages from 2 mo to 62 yr and found that HBsAg-specific CD8⁺ T cells decreased with age, which is consistent with the latest study reporting an age-related reduction of HBsAg-specific CD8⁺ T cells in CHB patients (Le Bert et al., 2020). Furthermore, we found that mMDSCs were negatively correlated with HBsAg-specific CD8⁺ T cells in infants and children but not in adults, indicating that mMDSCs might regulate HBsAg-specific CD8⁺ T cells in an age-related manner. Interestingly, we found that mMDSCs from CHB patients expressed a high level of CCR9, which classically mediates thymic recruitment of immune cells (Hadeiba et al., 2012). HBsAg was further proved to induce the expression of CCR9 on mMDSCs via activation of ERK1/2 and IL-6. These CCR9⁺ mMDSCs, carrying and cross-presenting HBsAg, could migrate to the thymic

[1]Key Laboratory of Medical Molecular Virology, School of Basic Medical Sciences, Shanghai Medical College of Fudan University, Shanghai, China; [2]Liver Cancer Institute of Zhongshan Hospital and Key Laboratory of Carcinogenesis and Cancer Invasion (Ministry of Education), Fudan University, Shanghai, China; [3]Shanghai Public Health Clinical Center, Shanghai Medical College of Fudan University, Shanghai, China; [4]Department of Infectious Diseases, Children's Hospital of Fudan University, Shanghai, China; [5]Program of Emerging Viral Diseases, Duke-NUS Medical School, Singapore; [6]Shanghai Frontiers Science Center of Pathogenic Microbes and Infection, Shanghai, China.

Prof. Hu died in 2017. Correspondence to Zhenghong Yuan: zhyuan@shmu.edu.cn; Zhong Fang: zhongfang13@fudan.edu.cn.

medulla and selectively eliminate HBsAg-specific CD8⁺ thymocytes, resulting in HBV persistence. We also found that blocking CCR9 with an antibody could efficiently inhibit the thymic migration of mMDSCs and could rescue HBsAg-specific CD8⁺ thymocytes, which results in breaking of HBV persistence.

As the thymus contributes to the generation of peripheral T cell repertoires and involutes with age (Buchholz et al., 2011), our finding uncovered a novel mechanism for establishing specific CD8⁺ tolerance to HBsAg via mMDSCs in infants and young patients after HBV exposure. This work raises a possibility that targeting mMDSCs or their migration should be a potential treatment for chronic HBV infection in infants and young patients, in whom the tolerance is not fully established.

Results

Expansion of mMDSCs correlates with a decrease in HBsAg-specific CD8⁺ T cells in young subjects with CHB

In previous study, we demonstrated that HBsAg-polarized mMDSCs can inhibit the activation of CD8⁺ T cells in vitro (Fang et al., 2015). Based on this work, we planned to evaluate the frequencies of mMDSCs and HBV-specific CD8⁺ T cells from CHB patients. To this end, patients were initially typed for HLAs. 16 out of 40 subjects, covering the ages from 2 mo to 62 yr, were identified as HLA-A2⁺ (Fig. S1 A), the most common HLA phenotype in populations. Core18-27 (HBcAg) and Env335-343 (HBsAg) are well-defined HLA-A2–restricted epitopes (Boni et al., 2007; Hoogeveen et al., 2019); therefore we examined HBsAg- and HBcAg-specific CD8⁺ T cells using MHC-1 tetramers based on these epitopes (Fig. S1 B). Results showed that the level of HBsAg-specific CD8⁺ T cells was dramatically lower than the level of HBcAg-specific CD8⁺ T cells, but both of them could be detected in at least some of the HLA-A2⁺ patients when comparing with values from HLA-A2⁻ samples (Fig. 1, A and B). In contrast, HLA-A2–restricted HPV E7 protein–specific CD8⁺ T cells were almost undetectable in HLA-A2⁺ subjects, as shown in Fig. S1 C.

A recent report showed that age was associated with HBsAg-specific CD8⁺ response (Le Bert et al., 2020). Analogously, we observed that the frequency of HBsAg-specific (Fig. 1 B), but not HBcAg-specific (Fig. 1 C) or HBV polymerase–specific (Fig. S1 D), CD8⁺ T cells was higher in young subjects compared with that in adults. In contrast, the level of cytomegalovirus (CMV) pp65–specific CD8⁺ T cells was higher in adults (Fig. S1 E). We further correlated age with HBV-specific CD8⁺ T cells. No correlation was found between HBcAg-specific CD8⁺ T cells and age ($R = -0.2057$, $P = 0.4448$, Fig. 1 E), but HBsAg-specific CD8⁺ T cells showed an inverse correlation with age ($R = -0.5821$ and $P = 0.018$, Fig. 1 D).

To assess the roles of mMDSCs in the regulation of HBV-specific CD8⁺ T cells, we analyzed the correlations between mMDSCs (HLA-DR$^{-/low}$CD33⁺CD11b⁺ CD14⁺) and HBV-specific CD8⁺ T cells and found that HBsAg-specific ($R = -0.5944$, $P = 0.0152$, Fig. 1 F), but not HBcAg-specific ($R = -0.01407$, $P = 0.9588$, Fig. 1 I), CD8⁺ T cells were inversely correlated with mMDSCs. As the frequency of HBsAg-specific CD8⁺ T cells was higher in young CHB patients (Fig. 1 B), we divided patients into two cohorts according to age and analyzed the correlations again. Interestingly, the inverse correlation was only observed in young patients ($R = -0.7566$, $P = 0.0298$, age ≤ 18, Fig. 1 G), but not in adult subjects ($R = -0.1014$, $P = 0.8112$, age > 18, Fig. 1 H). In contrast, we did not find any correlations between mMDSCs and HBcAg-specific CD8⁺ T cells in young patients ($R = 0.6375$, $P = 0.0981$, Fig. 1 J) or in adults ($R = -0.2353$, $P = 0.5784$, Fig. 1 K). Additionally, despite the level of mMDSCs being positively correlated with age ($R = 0.511$, $P = 0.043$, Fig. S1 F), this correlation was not observed after dividing the patients into two cohorts (Fig. S1, G and H). The reason might be that there are multiple factors contributing to the level of MDSCs, such as an increased risk of hepatocellular carcinoma in aged CHB patients and changes in hormones after adulthood. In summary, these results indicated that impairment of HBsAg-specific CD8⁺ T cells by mMDSCs operated differently in young patients and adults.

HBsAg induces expression of CCR9 on mMDSCs

The thymus contributes to the generation of peripheral T cell repertoires (Buchholz et al., 2011). In humans, thymic involution starts from as early as the first year of life, but a more rapid rate of attenuation starts from ages between 20 and 30 yr (Ackman et al., 2013). Immature dendritic cells (DCs) have been demonstrated to migrate into the thymus through CCR9 and regulate the negative selection of thymocytes (Bonasio et al., 2006; Hadeiba et al., 2012). Analogously, mMDSCs were also described as immature myeloid cell population (Condamine and Gabrilovich, 2011; Peranzoni et al., 2010). This raises a possibility that mMDSCs might participate in the development of HBsAg-specific CD8⁺ thymocytes.

To prove this, we detected the expression of CCR9 on mMDSCs. Since in healthy donors, almost all CD14⁺ cells are HLA-DR⁺, but not HLA-DR$^{-/low}$, mMDSC populations, we used total CD14⁺ myeloid cells as controls (Fang et al., 2015). The frequencies of CCR9⁺ cells and median fluorescence intensity (MFI) of CCR9 on CD14⁺ myeloid cells from CHB patients were significantly enhanced (Fig. 2 A), whereas there is no difference in MFI of CCR9 on CD14⁻ cells between these subjects (Fig. S2 A). We then analyzed peripheral blood mononuclear cells (PBMCs) from patients with chronic hepatitis C virus (HCV) and tuberculosis infections, in which MDSCs were also described to mediate immune suppression (Dorhoi and Du Plessis, 2017). CCR9 was slightly increased in chronic HCV patients, whereas it was dramatically enhanced in TB patients (Fig. S2 B). We then correlated CCR9 levels with clinical indicators in CHB patients ($n = 20$, Table S1). Serum HBsAg ($R = 0.5729$, $P = 0.0083$, Fig. 2 B), rather than hepatitis B e antigen (HBeAg; Fig. 2 C), HBV DNA (Fig. 2 D), alanine transaminase (ALT), or age (Fig. S2, C and D), showed a positive correlation with CCR9. Accordingly, after incubating with exogenous HBsAg (Chinese hamster ovary–derived, vaccine quality, adjuvant-free), expression of CCR9 was enhanced on CD14⁺ myeloid cells (Fig. 2 E), but not on T cells from healthy donors (Fig. S2 E). In contrast, exogenous HBeAg and OVA did not enhance CCR9 expression (Fig. S2, F and G). HBsAg-activated ERK1/2 and IL-6 have been demonstrated to promote polarization of mMDSCs from monocytes (Fang et al., 2015). We herein found that the ERK1/2 inhibitor or IL-6 neutralization antibody could efficiently block CCR9 expression mediated by HBsAg (Fig. 2 F).

Then, a persistent HBV strain plasmid, with a pUC18 backbone and HBV sequence derived–promoter (designated as BPS),

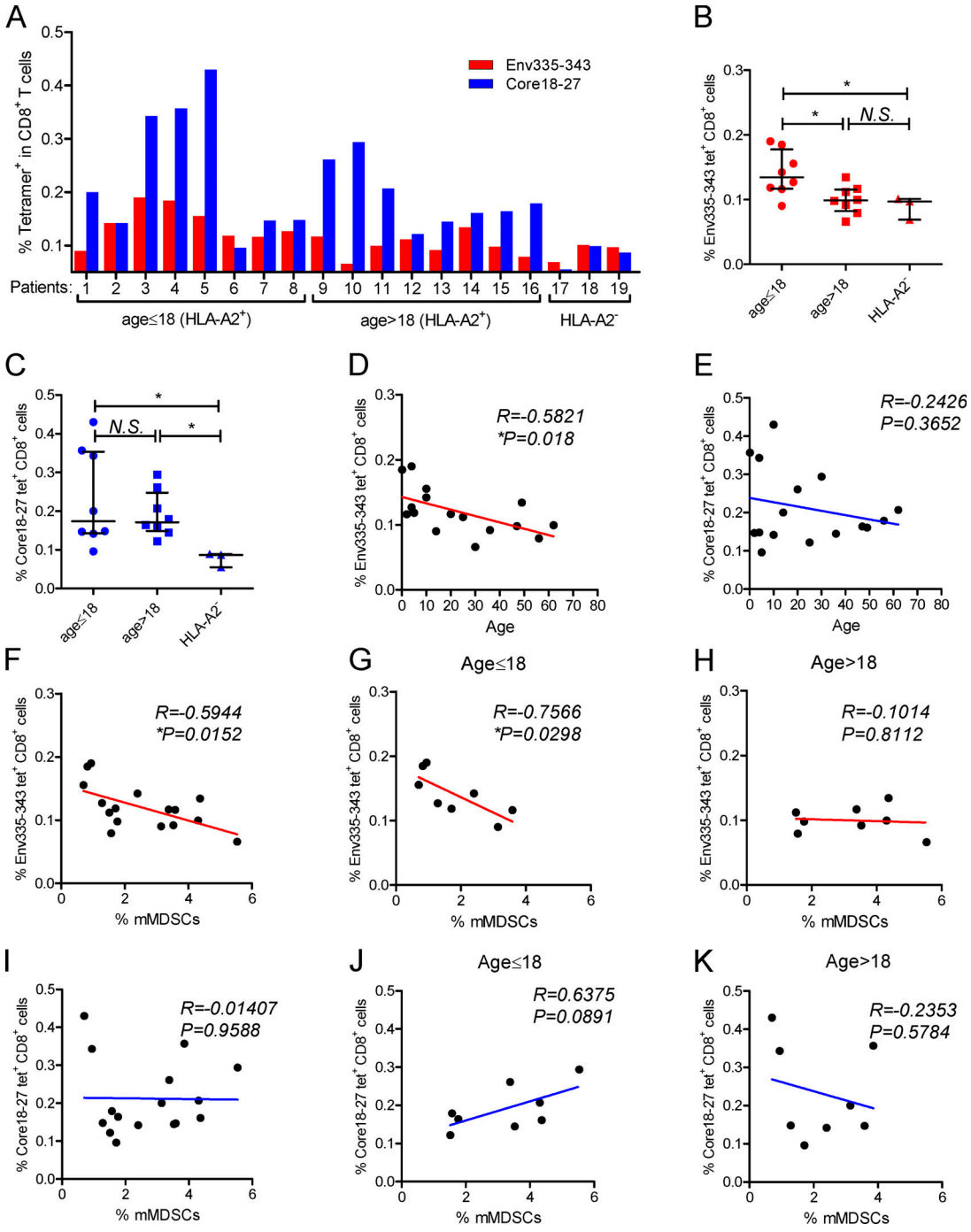

Figure 1. **Analysis of correlations between HBV-specific CD8⁺ T cells and mMDSCs or age. (A)** Analysis of HBV-specific CD8⁺ cells targeting HBsAg or HBcAg from HLA-A2⁺ CHB patients (n = 16). **(B and C)** Comparing the frequencies of HBsAg-specific (B) or HBcAg-specific (C) CD8⁺ T cells between subjects at different ages. **(D and E)** Correlating the age with HBsAg-specific (D) or HBcAg-specific CD8⁺ T cells (E; n = 16). **(F)** Correlating mMDSCs with HBsAg-specific CD8⁺ T cells in all subjects (n = 16). **(G and H)** Correlating mMDSCs with HBsAg-specific CD8⁺ T cells in subjects at age ≤ 18 (G) or age > 18 (H; n = 8). **(I)** Correlating mMDSCs with HBcAg-specific CD8⁺ T cells in all subjects (n = 16). **(J and K)** Correlating mMDSCs with HBcAg-specific CD8⁺ T cells in subjects at age ≤ 18 (J) or age > 18 (K; n = 8). *, P < 0.05.

as previously reported (Shen et al., 2017), was used to obtain HBV-persistent mice through hydrodynamic injection (HDI) of C57BL/6 mice. Murine mMDSCs were identified as the Gr1⁺Ly6C^{high}Ly6G⁻ population (Fang et al., 2015). We found that CCR9 was upregulated on mMDSCs in these HBV-persistent HDI mice compared with cells (defined with same markers) in naive mice (Fig. 2 G). In addition, the level of CCL25, a ligand of CCR9, was not altered in the thymus from these mice (Fig. S2 H). These results proved that HBsAg-activated ERK/IL-6 signaling also contributes to the expression of CCR9 on mMDSCs, indicating that induction of CCR9 and polarization of mMDSCs by HBsAg are simultaneous events.

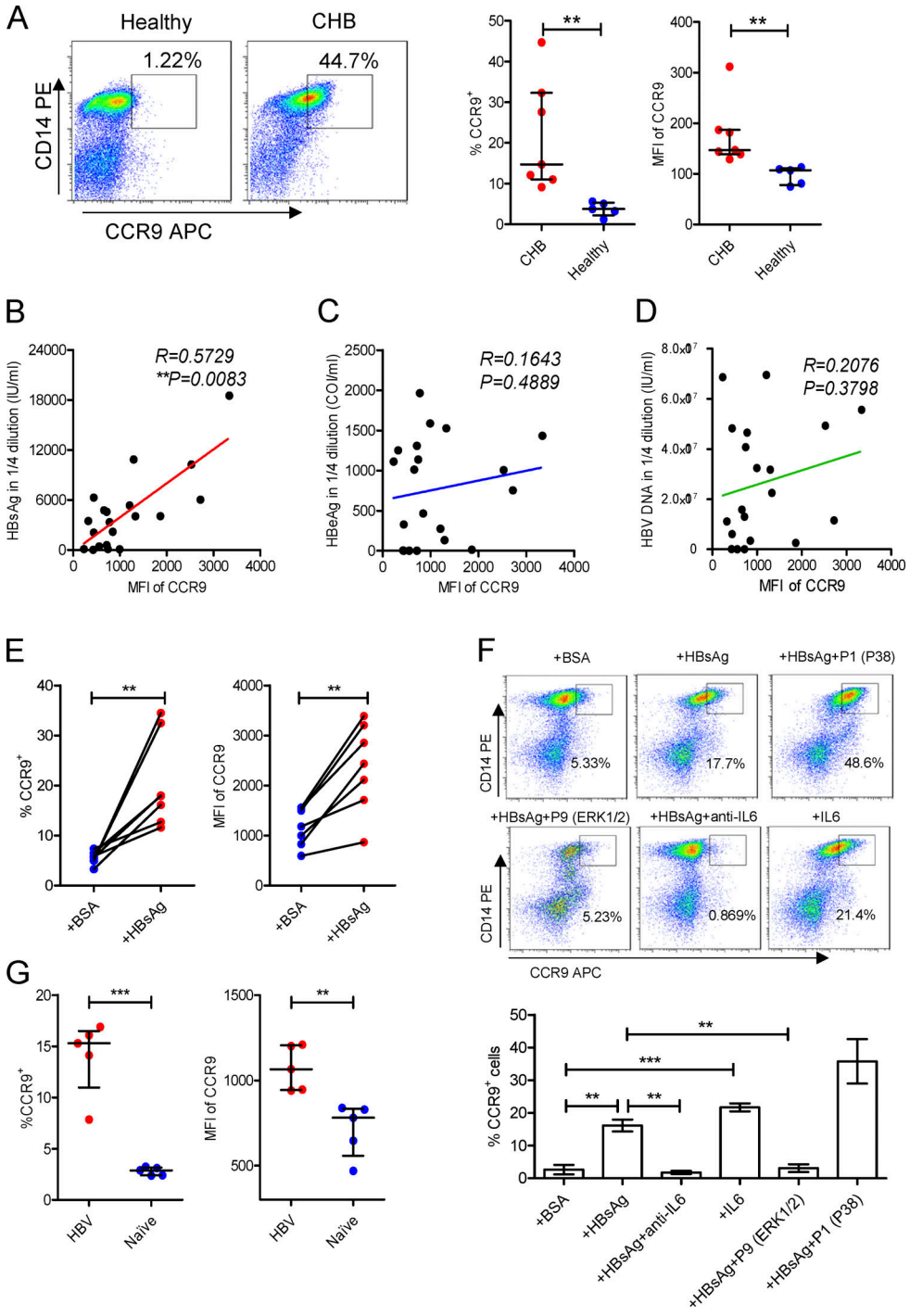

Figure 2. **Increase of CCR9 on mMDSCs. (A)** Flow cytometry staining of CCR9 on CD14⁺ myeloid cells from CHB patients (n = 7) or healthy donors (n = 5). **(B–D)** Correlating the median fluorescence intensity (MFI) of CCR9 with the levels of serum HBsAg (B), HBeAg (C), and HBV DNA (D) from CHB patients (age ≤ 18, n = 20). **(E)** Detecting CCR9 on exogenous HBsAg-stimulated CD14⁺ myeloid cells from heathy subjects (n = 7, 10 µg/ml). **(F)** Detecting HBsAg-induced CCR9 in the presence of inhibitors of P38, ERK1/2, and anti–IL-6 antibody (20 µg/ml) or exogenous IL-6 (5 ng/ml) without HBsAg (n = 3). **(G)** Detecting the level of CCR9 on endogenous mMDSCs from HBV-persistent HDI mice or naive mice (n = 5). **, P < 0.01; ***, P < 0.001.

Interaction between CCL25 and CCR9 mediates thymic homing of mMDSCs

We further investigated whether CCR9⁺ mMDSCs could be recruited by CCL25. A dose-dependent migration of mMDSCs from CHB patients was observed in a Transwell culture with human CCL25 (hCCL25), as shown in Fig. 3 A. In contrast, hCCL19 and hCXCL12 did not recruit mMDSCs (Fig. S3 A). Time-course assays of cultures of hCCL25-embedded agarose dots with purified mMDSCs (CFSE labeled) from patients confirmed this migration (Fig. 3 B). Using mouse CCL25 (mCCL25)–embedded agarose dots, we visualized the process of attraction of mMDSCs from HBV-persistent HDI mice (Fig. S3 B). Then, peripheral blood

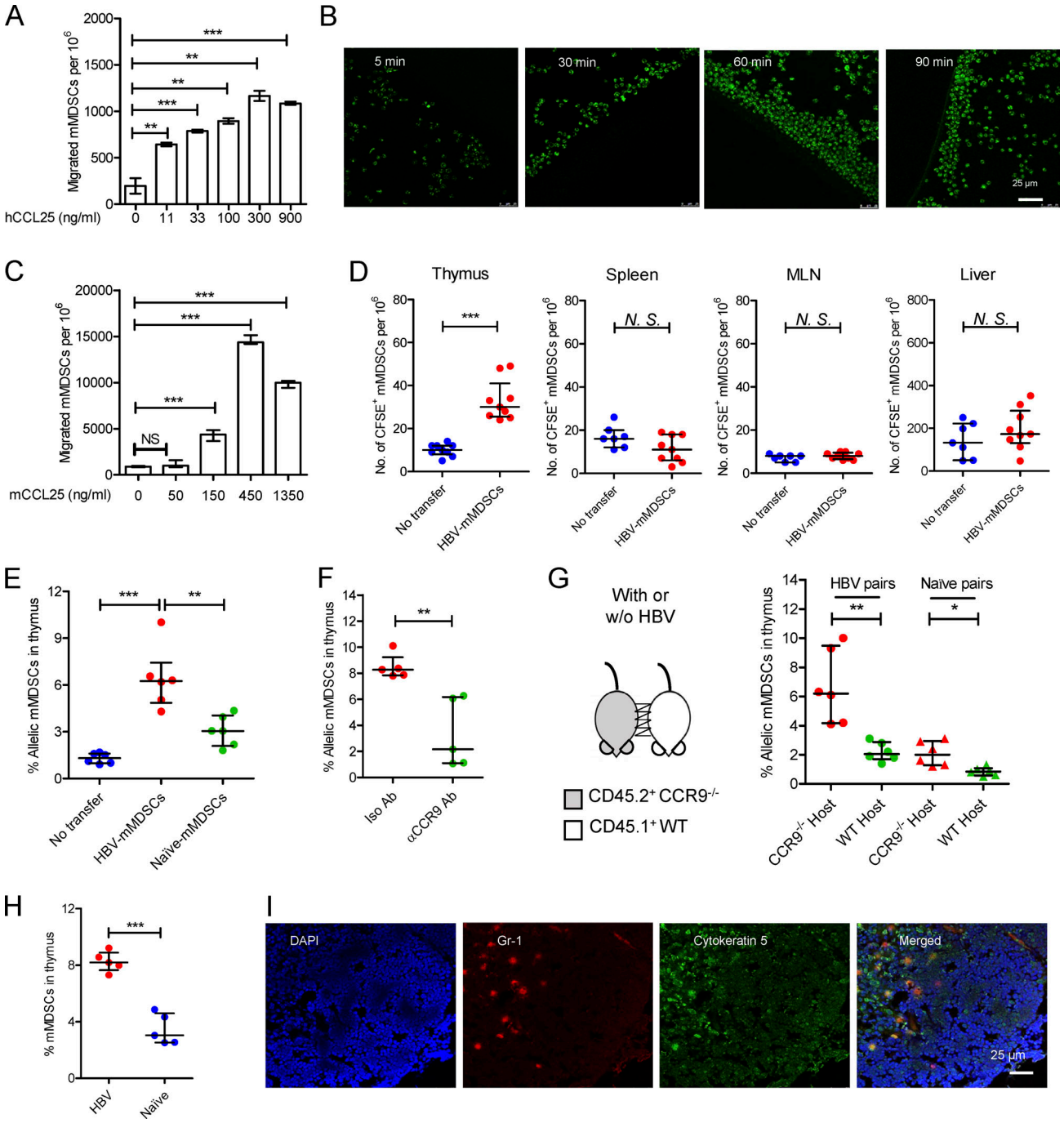

Figure 3. **Thymic homing of mMDSCs. (A)** Transwell migration study of mMDSCs from CHB patients toward hCCL25 (n = 3). **(B)** Time-course migration study of mMDSCs toward agarose dots containing hCCL25, triplicate. **(C)** Transwell migration study of PBLs from HBV-persistent HDI mice (n = 3). **(D)** Separately detecting mMDSCs in different tissues from naive mice at 36 h after ADT with CFSE-labeled mMDSCs from HBV-persistent HDI mice (10^7 cells per mice, n = 9). **(E)** Detecting allelic cells via flow cytometry after ADT of CD45.2+ HBV-persistent HDI– or naive mice–derived mMDSCs to CD45.1+ mice (n = 6). **(F)** Detecting mMDSCs in thymi of CD45.1+ mice after transfer of CCR9 antibody–blocked CD45.2+ mMDSCs (n = 5). **(G)** Detecting thymic allelic mMDSCs in pairs of WT and CCR9 knockout ($CCR9^{-/-}$) HBV or naive mouse pairs from parabiosis study (n = 6). **(H)** Detecting endogenous mMDSCs in the thymi from HDI-persistent HBV C57BL/6 mice (n = 5). **(I)** Location of endogenous mMDSCs in the thymi of HBV-persistent HDI mice. Nucleus (DAPI, blue), mMDSCs (Gr1, red), thymic medulla (cytokeratin-5, green), IF, triplicate. *, P < 0.05; **, P < 0.01; ***, P < 0.001.

leukocytes (PBLs) from HBV-persistent HDI mice were studied in Transwell. We found that mCCL25-responsive cells in PBLs expressed Gr1, the marker for mMDSCs, but not CD3 or CD19 (Fig. S3 C), and there was a dose-dependent migration for these cells (Fig. 3 C).

Mouse mMDSCs were then isolated through a magnetic activated cell sorting kit from Miltenyi Biotec, and purity was determined using flow cytometry (Fig. S3 D). We then adoptively transferred mMDSCs from HBV-persistent HDI mice to naive mice after labeling them with CFSE and found that a

significant number of mMDSCs existed in the thymus, rather than in the spleen, mesenteric lymph node, or the liver from the recipients (Fig. 3 D). Furthermore, we used allelic mice to confirm this migration. Transferring the same number of purified mMDSCs from CD45.2$^+$ HBV or naive mice to CD45.1$^+$ mice verified that HBV-persistent HDI mice–derived mMDSCs had a significantly stronger thymus-homing capability compared with cells from naive mice (Fig. 3 E), whereas blocking CCR9 with the antibody (9B1) inhibited this migration (Fig. 3 F). To investigate the thymic homing of endogenous mMDSCs from the periphery, we performed mice parabiosis. Detection of allelic PBLs verified the successful surgical operation (Fig. S3 E). In the pairs of CD45.1$^+$ WT and CD45.2$^+$ CCR9$^{-/-}$ HBV-persistent HDI mice, only few CD45.2$^+$ CCR9$^{-/-}$ mMDSCs migrated to the thymus of CD45.1$^+$ WT mice, whereas CD45.1$^+$ WT mMDSCs significantly increased in the thymus of the CD45.2$^+$ CCR9$^{-/-}$ counterparts (Fig. 3 G). In contrast, in naive mice pairs, the migration was limited (Fig. 3 G). Moreover, the migrated allelic Gr1$^+$ cells expressed Ly6C, but not CD11c, CD19, or Ly6G (Fig. S3 F), suggesting that they were mMDSCs but not DCs, B cells, or granulocytes.

Next, we studied thymic increase of mMDSCs in HBV-persistent HDI mice. The thymic mMDSCs in HBV-persistent HDI mice dramatically rose from 4 to 8% (Fig. 3 H). mMDSCs were also found to be located in the cytokeratin-5–positive thymic medulla (Fig. 3 I), the site for T cell negative selection. Additionally, adoptively transferred mMDSCs were also located in the thymic medulla (Fig. S3 G). These results indicated that mMDSCs were able to migrate into the thymic medulla from the periphery.

mMDSCs transfer HBsAg to mouse thymic medulla

MDSCs have been demonstrated to pick up and present tumor antigens to CD8$^+$ T cells (Kusmartsev et al., 2004; Nagaraj et al., 2007; Nagaraj et al., 2010). We herein observed that HBsAg was carried by mMDSCs from CHB patients (Fig. 4 A), corresponding to the report that HBsAg can only be internalized by peripheral CD14$^+$ myeloid cells (Gehring et al., 2013). In contrast, exogenous HBeAg could not be taken up by mMDSCs (Fig. S4 A). Using blocking antibodies, we further verified that this internalization was mediated by the mannose receptor (MR), rather than TLR2, TLR4, or CD14 (Fig. 4 B), which is supported by the finding that the MR contributes to internalization of HBsAg into DCs and macrophages (Wang et al., 2013).

We then observed that mMDSCs had increased expression of ubiquitin–proteasome subunits, including PSMA1, PSMA2, PSMC6, UPS12, and UBTD2, whereas MHC-II expression decreased (Fig. 4 C). HBsAg was also found to colocalize with PSMD1, a subunit of proteasome, but not with CD63, a marker for endosome (Fig. 4 D). A TCR-like antibody can bind to the complex of the HBsAg epitope and HLA-A2 (Env183/A2; Sastry et al., 2011). Using this antibody, we found that the level of Env183/A2 was significantly enhanced on HBsAg-induced (Fig. 4 E), but not on IL-6-induced, HLA-A2$^+$ mMDSCs polarized from healthy monocytes as reported in our previous work (Fang et al., 2015). In contrast, there was no difference in MFI of Env183/A2 between HBsAg-induced and IL-6–induced HLA-A2$^-$ mMDSCs (Fig. S4 B). Additionally, the level of this Env183/A2 complex, but not the Core18/A2 complex, on mMDSCs from HLA-A2$^+$ CHB patients was higher compared with that on control cells from healthy donors (Fig. S4, C and D). Ex vivo coculture also showed that HBV-persistent HDI mice–derived mMDSCs could promote death of HBsAg-TCR transgenic but not WT CD8$^+$CD4$^-$ thymocytes (Fig. 5 G), which was consistent with the report that DCs generated from HBsAg-carried CD14$^+$ myeloid cells could activate HBsAg-specific CD8$^+$ T cells (Gehring et al., 2013). These data suggested that mMDSCs could efficiently cross-present HBsAg via MHC-I.

We further determined whether mMDSCs can transfer HBsAg to the thymus and found that HBsAg was observed in endogenous thymic mMDSCs from HBV-persistent HDI mice via flow cytometry (Fig. 4 F) and immunohistochemistry (Fig. S4 E). In contrast, HBsAg is almost undetectable in the thymus of CCR9$^{-/-}$ HBV HDI mice (Figs. 4 G and S4 F). Importantly, HBsAg-carried mMDSCs were mainly located in the cytokeratin-8–negative area of the thymic medulla (Fig. 4 H). These results suggested that mMDSCs could transfer and cross-present HBsAg into the thymic medulla.

Thymic-homed mMDSCs promote death of HBsAg-specific CD8$^+$ thymocytes

Immune reconstitution with hematopoietic stem cells (HSCs) of mice allows us to investigate T cell deletion in the thymus (Hadeiba et al., 2012). We thereby reconstituted mice with mixed HSCs from HBsAg CD8$^+$-TCR transgenic and WT BALB/c mice. A graphic representation of the experimental steps is shown in Fig. 5 A. HBsAg-specific CD8$^+$ thymocytes were identified by MHC-I tetramer (Fig. 5 B). High dosage of the peptide (IPQSLDSWWTSL) was used as a positive control for thymocyte deletion (Bonasio et al., 2006). Results showed that transfer of mMDSCs from HBV-persistent HDI mice, rather than from naive mice, resulted in a decrease in HBsAg-specific CD8$^+$ thymocytes, whereas blocking CCR9 on mMDSCs with the antibody before transfer abolished this decrease (Fig. 5 C). Although OVA cannot enhance CCR9 (Fig. S2 G), we found that OVA-specific thymocytes in mice reconstitued with HSCs from OT-1 mice can also be eliminated after loading the OVA peptides onto mMDSCs from HBV subjects (Fig. S4 G). We were also able to visualize the physical contact of HBsAg-specific CD8$^+$ thymocytes and mMDSCs in the thymus from recipients (Fig. 5 D). Furthermore, cleaved caspase-3 could be detected in thymic tissues after transferring with mMDSCs (Fig. 5 E).

Ex vivo coculture of mMDSCs with HBsAg CD8$^+$-TCR transgenic thymocytes or peripheral T cells revealed that mMDSCs were able to promote the death of CD8$^+$CD4$^-$ thymocytes, but not peripheral CD8$^+$ T cells, in a dose-dependent manner (Fig. 5 F). We further verified that mMDSCs did not promote the death of CD8$^-$CD4$^+$, CD8$^+$CD4$^+$ (Fig. 5 G), or WT CD8$^+$CD4$^-$ thymocytes (Fig. 5 H). Cell death–related genes were also found to be upregulated in TCR transgenic CD8$^+$CD4$^-$ thymocytes after coculture with mMDSCs (Fig. 5 I). We previously demonstrated that NOX1 is upregulated in mMDSCs (Fang et al., 2015), and NOX1 is described to induce cell death (Kim et al., 2007). We herein found that the NOX1 inhibitor ML171 efficiently blocked the

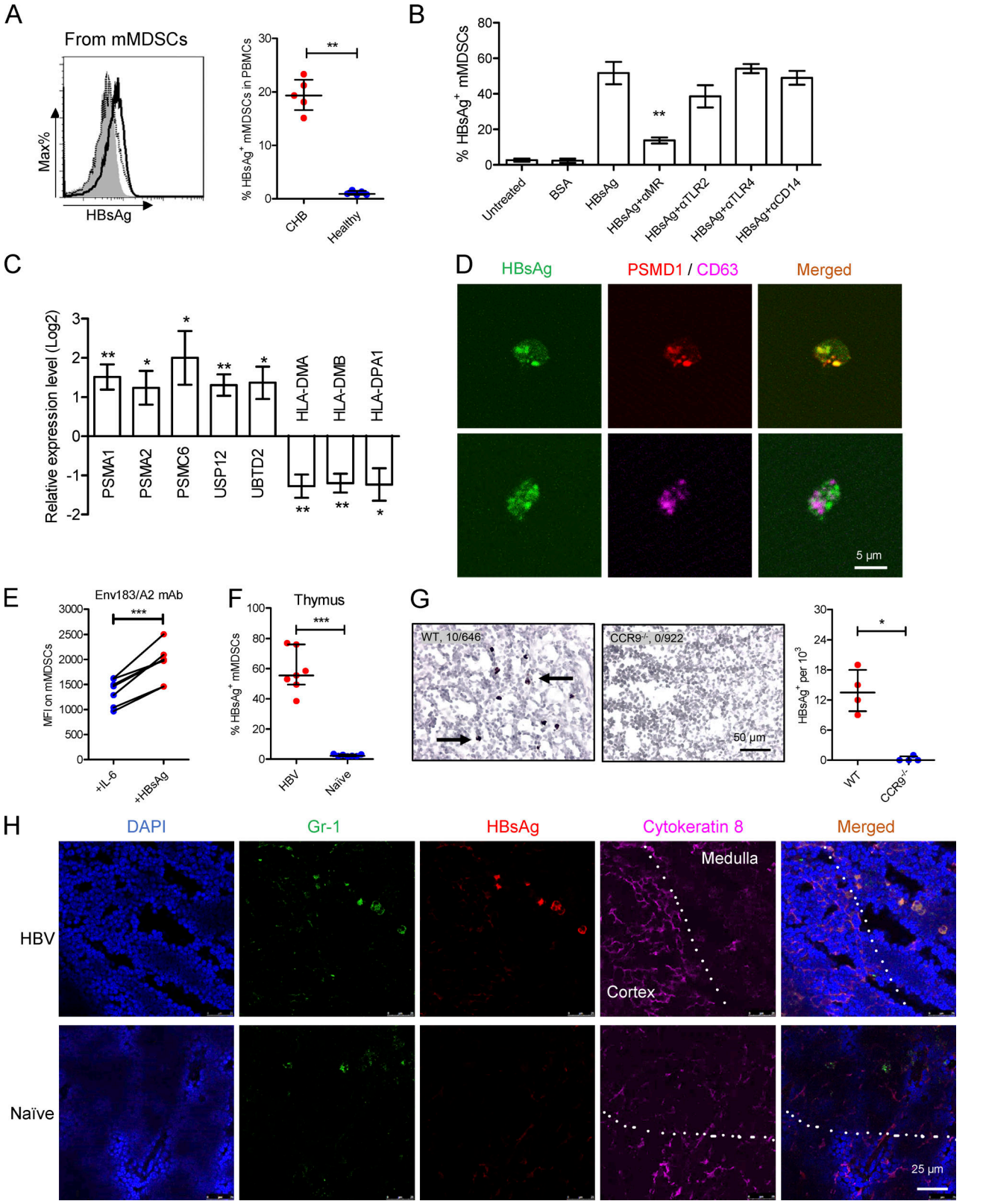

Figure 4. **mMDSCs transfer HBsAg to the thymic medulla. (A)** Intracellular staining of HBsAg in CD14$^+$ myeloid cells from CHB subjects (solid, n = 5) or healthy subjects (dotted, n = 5). **(B)** Detecting HBsAg in HBsAg-induced mMDSCs in the presence of blocking antibodies (n = 5, 20 μg/ml). **(C)** Levels of PSMA1, PSMA2, PSMC6, UPS12, UBTD2, HLA-DMA, HLA-DMB, and HLA-DPA1 in HBsAg-induced mMDSCs (n = 5). **(D)** Colocalization of intracellular HBsAg with PSMD1 or CD63 in mMDSCs. **(E)** Detecting the Env183/A2 complex on IL-6 or HBsAg-induced HLA-A2$^+$ mMDSCs with TCR-like antibody (n = 7). **(F)** Staining HBsAg in endogenous thymic mMDSCs from HBV-persistent HDI mice or naive mice (n = 7). **(G)** IHC staining HBsAg in thymi from WT or CCR9$^{-/-}$ HBV-persistent HDI mice. Arrows indicate the positive signaling in the IHC staining (brown, 400X, four views). **(H)** Localization of endogenous mMDSCs and HBsAg in the thymi of HBV-persistent HDI mice. Nucleus (DAPI), mMDSCs (Gr1), HBsAg, thymic cortex (cytokeratin-8), IF, triplicate. Dotted lines indicate the border of thymic cortex and medulla. *, P < 0.05; **, P < 0.01; ***, P < 0.001.

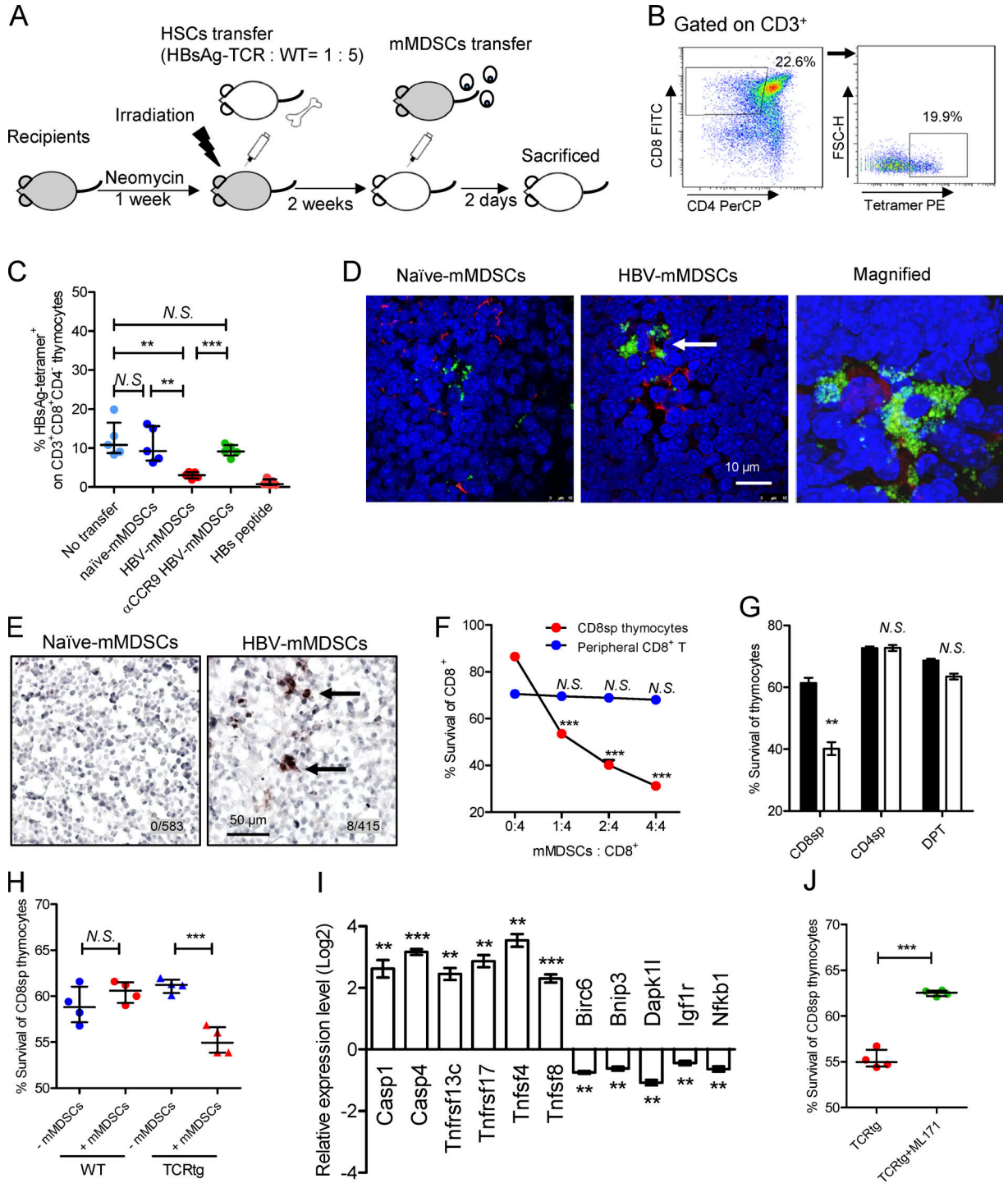

Figure 5. **mMDSCs promote death of HBsAg-specific CD8⁺ thymocytes. (A)** Experimental steps for immune reconstitution and adoptive transfer of mMDSCs. **(B)** Gating strategy for HBsAg-specific CD8⁺ thymocytes. **(C)** Detecting HBsAg-specific CD8⁺ thymocytes via flow cytometry in reconstituted mice on day 3 after transfer of mMDSCs (10^7 cells per mice, n = 5). **(D)** IF detection of colocalization of mMDSCs (Gr1, green) and HBsAg-specific CD8⁺ thymocytes (MHC-I tetramer, red) at 36 h after transfer of mMDSCs, triplicate. Arrows indicate the positive signaling in the IF detection. **(E)** Detecting cleaved caspase-3 in thymi of mice at 36 h after transfer of mMDSCs (brown, 400X), triplicate. Arrows indicate the positive signaling in the IHC staining. **(F)** Coculture of HBV-persistent HDI mice–derived mMDSCs (effector, E) with CD8⁺CD4⁻ (CD8sp) thymocytes or peripheral CD8⁺ T cells (target, T) from HBsAg-TCR transgenic mice for 18 h. Detection of Annexin V and 7-ADD double negative cells (n = 5). **(G)** Coculture of naive (empty) mice– or HBV-persistent HDI (filled) mice–derived mMDSCs with HBsAg-TCRtg thymocytes (E: T = 1: 2; n = 4). **(H)** Coculture of HBV-persistent HDI mice–derived mMDSCs with thymocytes from WT or HBsAg-TCRtg mice (E: T = 1: 2; n = 4). **(I)** Levels of genes related to cell death in HBsAg-TCRtg CD8⁺CD4⁻ thymocytes after coculture with HBV-persistent HDI mice–derived mMDSCs (5 h). **(J)** Coculture of HBV-persistent HDI mice–derived mMDSCs with TCRtg CD8⁺CD4⁻ thymocytes in the presence of 5 μM NOX1 inhibitor (ML171). **, P < 0.01; ***, P < 0.001.

death of HBsAg-specific CD8⁺CD4⁻ thymocytes cocultured with mMDSCs (Fig. 5 J). Taken together, these results suggested that mMDSCs from HBV-persistent HDI mice could promote the death of HBsAg-specific CD8⁺CD4⁻ thymocytes.

CCR9 blocking interrupts the effects of mMDSCs

To study the impact of deletion of HBsAg-specific CD8⁺ thymocytes on anti-HBV immune responses, we reconstituted CD45.2⁺ mice with CD45.1⁺ HSCs following with adoptive transfer of mMDSCs (10^7 cells per mice, 14 d after reconstitution) and immunized them with pcDNA3.1-HBsAg plasmid or OVA protein at week 4 after transfer. The frequencies of IFN-γ–positive CD8⁺ T cells (HBsAg peptide-stimulated) and HBsAg-specific CD8⁺ T cells could be efficiently detected in the spleen of vaccinated mice, whereas mMDSCs from HBV-persistent HDI mice impeded the response and level of HBsAg-specific CD8⁺ T cells (Fig. 6, A and B). Importantly, CCR9-blocked mMDSCs lost the capability to regulate HBsAg-specific CD8⁺ T cells as expected (Fig. 6, A and B). Conversely, mMDSCs did not alter the frequency of OVA-specific CD8⁺ T cells (Fig. 6 C).

Thymic sides peak at 4–6 wk of age in the mice (Aw et al., 2007); therefore, we performed HDI on 3–4-wk-old mice or 7–8-wk-old mice with an HBV B6 strain, which could be rapidly eliminated in adult mice (Shen et al., 2017). As expected, this HBV model is characterized by age-related viral persistence and HBsAg-specific CD8⁺ T cell generation (Fig. 6, D and E), whereas the level of ALT and generation of HBcAg-specific CD8⁺ T cells were not related to age (Fig. 6, F and G). To determine the contribution of mMDSCs to viral persistence and generation of HBsAg-specific CD8⁺ T cells, mMDSCs were transferred into naive 4-wk-old C57BL/6 mice, and then, these mice were hydrodynamically injected with the HBV B6 plasmid when they were 7 wk old. In mMDSC-transferred mice, HBsAg-specific CD8⁺ T cells were significantly lower (Fig. 6 H), and the duration of HBsAg in serum was much longer (Fig. 6 I). Notably, CCR9-blocked mMDSCs did not change the frequency of T cells and viral persistence (Fig. 6, H and I). These data suggested that mMDSCs selectively obliterated peripheral HBsAg-specific CD8⁺ T cells and facilitated HBsAg persistence in a CCR9-dependent manner.

Discussion

Children are able to mount virus-specific T cell responses toward different kinds of viral infections (Hong and Bertoletti, 2017). Accordingly, vaccination in infants can activate protective immune responses to HBV (Li et al., 2018), but HBV exposure in infants easily leads to chronic infection. The mechanism underlying these conflicting phenomena is not clear. A study showing that maternal HBeAg crosses the placenta and suppresses T cell response gives an explanation for this (Tian et al., 2016), but loss of HBeAg accompanied by the activation of HBeAg/HBcAg-specific CD8⁺ T cells usually occurs in most of CHB patients without HBV cure (Cheng et al., 2019; Matsumura et al., 2001). Interestingly, HBsAg-specific CD8⁺ T cells, preferentially undetected in CHB adults (Hoogeveen et al., 2019; Rivino et al., 2018), are convincingly shown to play a pivotal role in HBV clearance (Nitschke et al., 2016; Thimme et al., 2003). Although MDSCs in CHB have been described to inhibit CD8⁺ T cell activation in vitro (Fang et al., 2015; Yang et al., 2019), this does not explain the age-related outcome of HBV exposure. Importantly, MDSCs have been found to be critical for the control of inflammation in neonates (He et al., 2018). We herein demonstrated that HBsAg-specific CD8⁺ T cells were eliminated by mMDSCs before their release from the thymus. Notably, bone marrow cellularity declines, and the thymus involutes as early as the first year of life in humans and loses its function in adults (Hakim and Gress, 2007; Thapa and Farber, 2019). Studies have showed there are two rapid decreasing periods of thymic T cell output. One is between the ages of 0 and 5 yr, and another is between the ages of 20 and 30 yr (Ye and Kirschner, 2002). Similarly, from infancy to age 5, the chronicity upon exposure to HBV decreases precipitously occurring at 90–50%, respectively. Therefore, mMDSC-mediated deletion of antigen-specific CD8⁺ thymocytes should operate differently in HBV-exposed adults and children.

Progression of CHB is known as natural history, which is usually classified into five phases, including HBeAg-positive chronic infection, HBeAg-positive chronic hepatitis, HBeAg-negative chronic infection, HBeAg-negative chronic hepatitis, and HBsAg-negative phase (European Association for the Study of the Liver, 2017). In the beginning phase, after HBV exposure, there is almost no inflammation in livers, which results in peripheral immune cells being difficult to migrate into livers. Nevertheless, substantial HBsAg in circulation could modify the phenotype and function of immune cells, such as monocytes (Fang et al., 2015). Our previous work showed that without multiple cooperation of other cytokines, HBsAg-induced IL-6 could contribute to polarization of mMDSCs and upregulation of CCR9 on mMDSCs, which was supported by the finding that IL-6 could promote CCR9 expression on monocytes (Rolin et al., 2014). CCL25, the only ligand for CCR9, is secreted by the intestine under inflammation (Trivedi et al., 2016) and by the thymus under normal conditions (Vicari et al., 1997), which means that although there is no inflammation in the beginning phase of CHB, CCR9⁺ mMDSCs could still be recruited into the thymus. Similarly, Tregs expressing CCR9 are capable of homing to the intestines with respect to CCL25, demonstrating alternative phenotypic fates dependent on IL-6 signaling (Ma et al., 2019). Besides, we also found enhancements of CCR2 (data not shown), which might help mMDSCs home to the liver in the later hepatitis phase of CHB.

Clonal deletion of T cells in the thymus is known as central tolerance. Cross-presentation of tissue-restricted self-antigens by resident DCs was shown to mediate CD8⁺ thymocyte selection (Koble and Kyewski, 2009; Lancaster et al., 2019). Nevertheless, it remains unclear whether antigen-specific CD8⁺ T cell precursors could be deleted by transporting antigen from periphery to the thymus, whereas thymic-homed DCs and B cells only mediate negative selection of CD4⁺ thymocytes (Lopes et al., 2015; Yamano et al., 2015). Our finding provides direct evidence that HBV was able to hijack thymic tolerance and alter the peripheral CD8⁺ repertoires through polarizing thymic-recruited mMDSCs. We demonstrated that peripheral mMDSCs could take

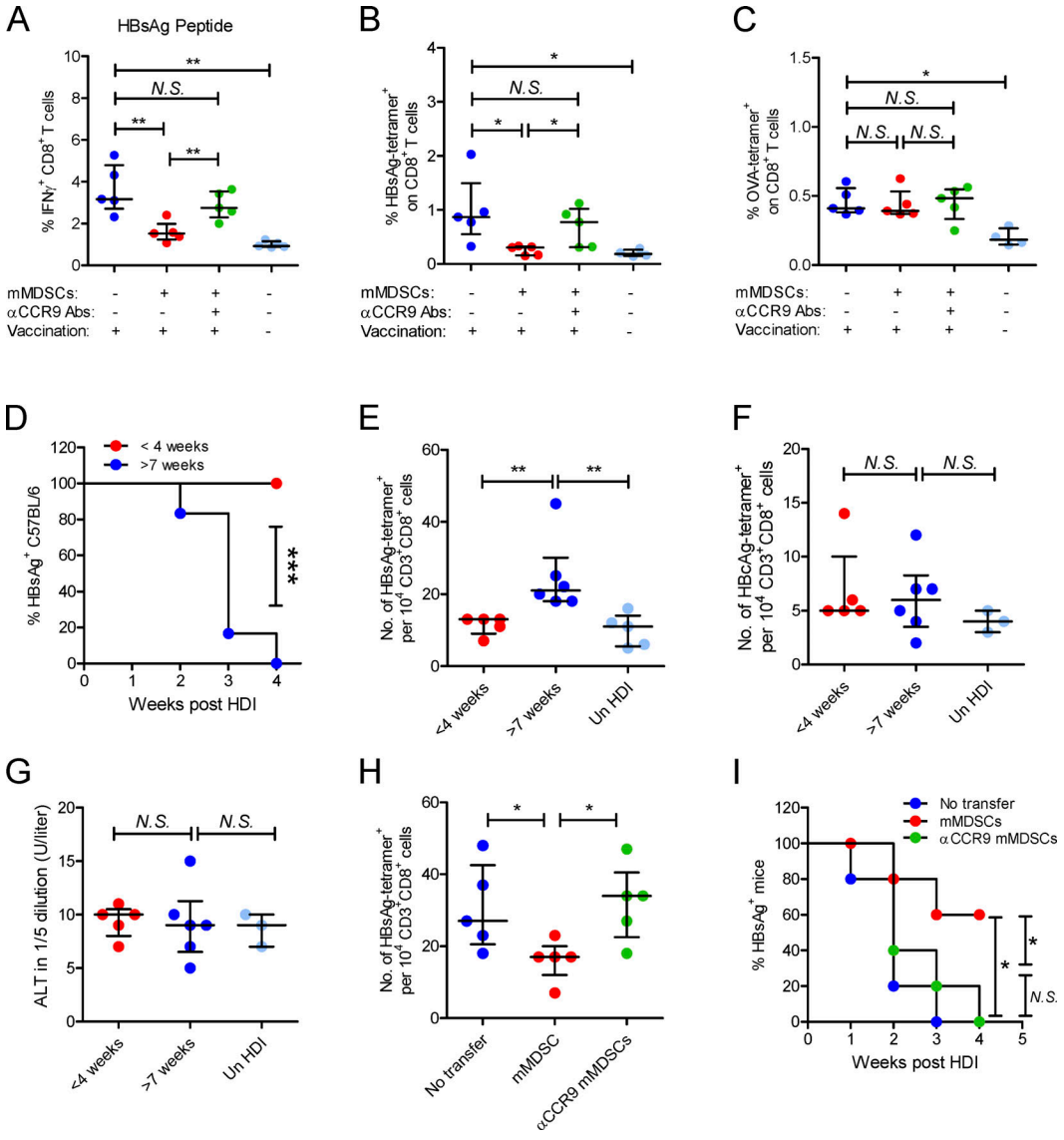

Figure 6. **mMDSCs mediate HBsAg-specific CD8⁺ T cell deletion and HBsAg persistence through CCR9. (A)** Intracellular staining IFN-γ–positive CD8⁺ T cells in HBsAg peptide-stimulated (5 µg/ml) PBLs from HBsAg-vaccinated mice after transfer of HBV-persistent HDI mice–derived mMDSCs (n = 5). **(B)** Detecting HBsAg-specific CD8⁺ T cells with the MHC tetramer in splenocytes of HBsAg-vaccinated mice (n = 5). **(C)** Detecting OVA-specific CD8⁺ T cells in splenocytes of OVA-vaccinated mice after transfer of HBV-persistent HDI mice–derived mMDSCs (n = 5). **(D)** Persistence of serum HBsAg in C57BL/6 mice with different ages (n = 6). **(E–G)** The levels of HBsAg-specific CD8⁺ T cells (E), HBcAg-specific CD8⁺ T cells (F), and ALT (G) in C57BL/6 mice with different ages, day 10 after HDI of HBV B6 strain (n = 5). **(H)** Level of HBsAg-specific CD8⁺ T cells in mice after pretransfer of HBV B6 HDI mice–derived mMDSCs (n = 5). **(I)** Persistence of serum HBsAg in mice with pretransfer of mMDSCs (n = 5). *, P < 0.05; **, P < 0.01.

up HBsAg through the MR and transfer it to the thymus. The MR has been reported to mediate antigen internalizing into cytosol for proteasomal degradation and cross-presentation (Zehner and Burgdorf, 2013), which is consistent with our finding that HBsAg could be cross-presented by mMDSCs. To investigate cross-presentation of HBsAg, we first observed the colocalization of HBsAg and a subunit of proteasome (PSMD1), the site for generating peptides presented on MHC-I (Zehner and Burgdorf, 2013). Testing activation of antigen-specific CD8⁺ T cells cocultured with DCs or macrophages is most powerful method to explore antigen cross-presentation (Gehring et al., 2013). However, mMDSCs do not activate CD8⁺ T cells. We therefore examined death instead of activation of HBsAg-specific CD4⁻CD8⁺ thymocytes after coculture with mMDSCs, which also offered testimony for the cross-presentation. Beyond this, we examined the complex of MHC-I and the HBsAg epitope (Env183/A2) on mMDSCs using a TCR-like antibody, providing direct evidence for the cross-presentation.

A number of studies have demonstrated that human immunodeficiency virus–, simian immunodeficiency virus (SIV)–, lymphocytic choriomeningitis virus–, CMV-, Epstein–Barr virus–, and *Mycobacterium tuberculosis*–associated chronic infections have detrimental effects on the thymic function (Nunes-Alves et al., 2013). However, none of them has been demonstrated to directly regulate CD8⁺ thymocytes so far. In this study, we observed that mMDSCs promoted the death of CD8⁺

thymocytes rather than peripheral CD8⁺ T cells, although mMDSCs have been well studied in restraining their activation. The next question will be how mMDSCs acquire the capability to eliminate CD8⁺ thymocytes. iNOS, NOX2, and PD-L1 all are found to affect both thymic negative selection (Aiello et al., 2000; Daley et al., 2013) and MDSC-mediated T cell suppression (Condamine and Gabrilovich, 2011; Corzo et al., 2009; Lechner et al., 2010; Lechner et al., 2011). Accordingly, we found an enhanced expression of NOX2 in HBsAg-polarized mMDSCs (Fang et al., 2015). Moreover, we detected the cleavage of caspase-3 and NOX1, indicating that mMDSCs could promote the death of thymocytes via NADPH oxidase. The most likely reason for the different effects of mMDSCs to peripheral CD8⁺ T cells and CD8⁺ thymocytes should be distinct level of Bcl-2. Bcl-2 has been reported to inhibit cell death, and thymocytes express less Bcl-2 compared with peripheral T cells (Veis et al., 1993). Bcl-2 has also been shown to help in the survival of peripheral CD8⁺ T cells (Kurtulus et al., 2011) and prevent cell damage induced by NOX1 (Zanetti et al., 2014). We believe this mechanism deserves further investigation.

Recently, interruption of recruitment of immune suppressor cells has been suggested as an efficient strategy for therapy. Anti-CCL2 antibody can block recruitment of tumor-associated macrophage and breakdown of immunological tolerance in prostate cancer (Izhak et al., 2010). Disruption of CCR5 on regulatory T cells can benefit mice with pancreatic cancer (Tan et al., 2009). Similarly, our data from HBV model mice demonstrated that neutralization of CCR9 was able to block thymic homing of mMDSCs and disrupt effects of mMDSCs on deletion of HBsAg-specific CD8⁺ thymocytes, which resulted in the persistence of HBV being interrupted. This raises a potential strategy for CHB treatment through selectively interfering or neutralizing CCR9 on mMDSCs.

As we provide insight into a novel mechanism that HBV eliminates HBsAg-specific CD8⁺ thymocytes through mMDSCs, the pharmacological interference of mMDSCs or their migration toward the thymus might represent a new approach of anti-HBV therapies, and the better age for HBV therapies should be as young as possible. Besides that, this study also gives direct evidence that chronic infection of HBV could affect development of antigen-specific CD8⁺ thymocytes.

Materials and methods

Human subjects

Peripheral blood samples were collected from CHB patients (positive for HBeAg, HBsAg, and HBV-DNA) who were not receiving any therapy in the past 6 mo. Patients with other infections, autoimmune hepatitis, or tumors were excluded. HBsAg, HBeAg, HBV DNA, and ALT were measured in the Clinical Laboratory of the Shanghai Public Health Clinical Center. Healthy PBMCs from anonymous donors were provided by the Red Cross Blood Center of Shanghai, China. The Ethics Committee of the Shanghai Public Health Clinical Center approved the use of peripheral blood samples from all human subjects, and we have obtained informed consent from all participants.

Mice

BALB/c and C57BL/6 (CD45.2) mice were purchased from Super-B&K Laboratory Animal Corp. Ltd. C57BL/6-congenic CCR9$^{-/-}$ mice (No. 027041) and BALB/c-congenic HBsAg-TCR transgenic mice (No. 027510) were purchased from The Jackson Laboratory. A volume of 5 μg of BPS or B6 plasmid in PBS equivalent to 8% of the body weight was hydrodynamically injected into the tail vein of C57BL/6 or BALB/c mice to establish an HBV replication model. All mice were housed and bred under specific pathogen–free conditions according to the protocol approved by the Ethics Committee of the Shanghai Public Health Clinical Center.

MHC-I tetramers

HLA-A2–restricted HPV E7 11-19 peptide or HBV peptides, including Pol455-463 (polymerase), Core18-27 (HBcAg), Env335-343 (HBsAg), and Flex-T HLA-A*02:01 Monomer UVX (BioLegend), were used to prepare MHC-I tetramers. APC H-2Kb HBsAg190-197 (VWLSVIWM) and PE H-2Ld HBsAg28-39 (IPQSLDSWWTSL) MHC-I tetramers were purchased from HelixGen Corp. Ltd.

Flow cytometry

The following antibodies were purchased from BD Pharmingen: anti-human CD3 PE (HIT3a), anti-human CD4 FITC (RPA-T4), anti-human CD8α APC (RPA-T8), and anti-human IFN-γ FITC (S. B3). The following antibodies were purchased from BioLegend: anti-human HLA-DR APC-CY7 (L243), anti-human CD3 Brilliant Violet 421 (UCHT1), anti-human CD4 APC-CY7(RPA-T4), anti-mouse CD3 APC-CY7 (17A2), anti-mouse CD4 PerCP (GK1.5), and anti-mouse CD8α FITC (53-6.7). The following antibodies were purchased from eBioscience: anti-human HLA-A2 APC (BB7.2), anti-mouse IFN-γ APC (XMG1.2). TCR-like antibodies targeting Env183/A2 and Core18/A2 were used to detect HLA-A2/peptide complexes on mMDSCs. TCR-like antibodies (10 μg/ml) were first incubated with cells for 1 h, and then, AF647 goat anti-mouse IgG (minimal x-reactivity, BioLegend) was added for further 30 min incubation. All samples were analyzed with BD LSR Fortessa.

Immunofluorescence and immunohistochemistry

Mouse thymi were cut into 8 μm frozen sections using a Leica CM1520 cryostat (Leica Biosystems). Anti-mouse Gr1 and anti-mouse CD45.2 were purchased from BioLegend. Anti-mouse cytokeratin 5, anti-mouse cytokeratin 8, anti-HBsAg, and anti-HBsAg were from Bioss Inc. H-2Ld HBsAg28-39 (IPQSLDSWWTSL) MHC-I tetramer (PE) was used to detect HBsAg-specific CD8⁺ thymocytes in the immunofluorescence (IF) test.

Migration assays

Mouse mMDSCs (Gr1⁺Ly6C^{high}Ly6G⁻) were isolated using an MDSC isolation kit (Miltenyi Biotec), and human mMDSCs (HLA-DR$^{-/low}$CD33⁺CD11b⁺ CD14⁺) were isolated through flow cytometry sorting. Approximately 10^6 PBLs, PBMCs, or purified mMDSCs from CHB mice or patients were placed in the upper chamber insert (8 μm pores) of Transwell inserts (Cat. 3422; Corning), and CCL25 was added to the lower chambers. After 3 h

of incubation, cells in the lower wells were analyzed by flow cytometry. In agarose dot assay, murine or human CCL25 (BioLegend) was added to molten 0.5% agarose solution at 40°C, and a drop was pipetted onto the base of a sterile 20-mm-diameter glass-bottomed 8-well chambered cell culture slide (MatTek Corporation).

Adoptive transfer and parabiosis

In adoptive transfer, mouse mMDSCs were isolated as mentioned above and i.v. injected into recipient mice. Recipients were sacrificed at 36 h after transfer. For parabiosis, mice were anesthetized to attain full muscle relaxation and were joined. 2 wk after parabiosis, mouse thymi were analyzed.

Immune reconstitution

Recipients were irradiated with 9 Gy (C57BL/6) or 8 Gy delivered in two episodes separated by 4 h (BALB/c; Cui et al., 2002; Wang et al., 2018). HSCs were isolated using a MojoSort mouse HSC isolation kit (BioLegend). A mixture of HSCs from WT and HBsAg-TCR or OVA-TCR transgenic donors (5:1) were i.v. injected into irradiated recipients (10^5 HSCs per mouse). On days 14 and 15 after HSCs transfer, mice were injected with two doses of mMDSCs. Anti-CCR9 blocking Ab (50 µg/ml, clone: 9B1; BioLegend) was used to block CCR9 on mMDSCs before transfer (Rivera-Nieves et al., 2006). On day 3 after the first mMDSC transfer, mice were sacrificed.

Statistical analysis

Data were analyzed using GraphPad Prism 5. Statistical significance was assessed by Mann–Whitney test or unpaired/paired two-tailed *t* tests. Nonparametric correlations between two continuous variables were tested using the coefficient of determination, R. Error bars in figures presented the median with interquartile range. *, P < 0.05; **, P < 0.01; ***, P < 0.001.

Online supplemental material

Fig. S1 shows analysis of antigen-specific $CD8^+$ cells in PBMCs from CHB patients, including gating strategy, frequencies, and correlations. Fig. S2 shows analysis of chemokine receptors on mMDSCs and other cells from patients or antigen-stimulated PBMC cultures. Fig. S3 shows migration of mMDSCs toward different chemokines and their thymic homing capability in parabiosis assay. Fig. S4 shows antigen transfer and OVA-specific $CD8^+$ thymocytes deletion by mMDSCs. Table S1 shows basic clinical information of the studied patients.

Acknowledgments

We would like to dedicate this paper to Professor Yunwen Hu, who unfortunately passed away before this paper was submitted. Yunwen played an essential role in the early stage of this study, and she is greatly missed. We thank Q. Leng from the Institute Pasteur of Shanghai for providing $CD45.1^+$ C57BL/6 mice and J. Xu from the Shanghai Public Health Clinical Center for providing OT-1 mice.

This study was funded by the National Key R&D Program of China (No. 2021YFC2300602 to Z. Yuan), the National Natural Science Foundation of China (No. 91842309 to Z. Yuan), the Research Unit of Chronic Hepatitis B virus infection from China Academy of Medical Science (No. 2019RU037 to Z. Yuan), the Local Innovative and Research Teams Project of Guangdong Pearl River Talents Program (No. 2017BT01S131 to Z. Yuan), and the National Natural Science Foundation of China (No. 81471931 to Y. Hu).

Author contributions: Z. Yuan, Z. Fang, and Y. Hu designed the experiments. Z. Fang, J. Li, and M. Kozlowski prepared the figures and/or wrote the manuscript. Y. Zhang, Z. Zhu, Y. Hu, D. Zhang, J. Zhao, and H. Yu collected clinical samples from patients. Z. Fang, C. Wang, B. Shi, and A. Bertoletti performed and/or analyzed ex vivo and in vitro experiments. Z. Fang, C. Wang, X. Peng, Z. Shen, M. Wu, C. Xu, X. Zhou, and Y. Xie performed and/or analyzed in vivo experiments. A. Bertoletti, J. Chen, and X. Zhang gave suggestions in the experiments.

Submitted: 30 August 2021
Revised: 2 December 2021
Accepted: 31 January 2022

References

Ackman, J.B., B. Kovacina, B.W. Carter, C.C. Wu, A. Sharma, J.A.O. Shepard, and E.F. Halpern. 2013. Sex difference in normal thymic appearance in adults 20-30 years of age. *Radiology*. 268:245–253. https://doi.org/10.1148/radiol.13121104

Aiello, S., M. Noris, G. Piccinini, S. Tomasoni, F. Casiraghi, S. Bonazzola, M. Mister, M.H. Sayegh, and G. Remuzzi. 2000. Thymic dendritic cells express inducible nitric oxide synthase and generate nitric oxide in response to self- and alloantigens. *J. Immunol.* 164:4649–4658. https://doi.org/10.4049/jimmunol.164.9.4649

Aw, D., A.B. Silva, and D.B. Palmer. 2007. Immunosenescence: emerging challenges for an ageing population. *Immunology*. 120:435–446. https://doi.org/10.1111/j.1365-2567.2007.02555.x

Bertoletti, A., and P.T.F. Kennedy. 2019. HBV antiviral immunity: not all CD8 T cells are born equal. *Gut*. 68:770–773. https://doi.org/10.1136/gutjnl-2018-317959

Bonasio, R., M.L. Scimone, P. Schaerli, N. Grabie, A.H. Lichtman, and U.H. von Andrian. 2006. Clonal deletion of thymocytes by circulating dendritic cells homing to the thymus. *Nat. Immunol.* 7:1092–1100. https://doi.org/10.1038/ni1385

Boni, C., P. Fisicaro, C. Valdatta, B. Amadei, P. Di Vincenzo, T. Giuberti, D. Laccabue, A. Zerbini, A. Cavalli, G. Missale, A. Bertoletti, et al. 2007. Characterization of hepatitis B virus (HBV)-specific T-cell dysfunction in chronic HBV infection. *J. Virol.* 81:4215–4225. https://doi.org/10.1128/JVI.02844-06

Boonstra, A., A.M. Woltman, and H.L.A. Janssen. 2008. Immunology of hepatitis B and hepatitis C virus infections. *Best Pract. Res. Clin. Gastroenterol.* 22:1049–1061. https://doi.org/10.1016/j.bpg.2008.11.015

Buchholz, V.R., M. Neuenhahn, and D.H. Busch. 2011. CD8+ T cell differentiation in the aging immune system: until the last clone standing. *Curr. Opin. Immunol.* 23:549–554. https://doi.org/10.1016/j.coi.2011.05.002

Cheng, Y., Y.O. Zhu, E. Becht, P. Aw, J. Chen, M. Poidinger, P.F. de Sessions, M.L. Hibberd, A. Bertoletti, S.G. Lim, and E.W. Newell. 2019. Multifactorial heterogeneity of virus-specific T cells and association with the progression of human chronic hepatitis B infection. *Sci. Immunol.* 4:eaau6905. https://doi.org/10.1126/sciimmunol.aau6905

Condamine, T., and D.I. Gabrilovich. 2011. Molecular mechanisms regulating myeloid-derived suppressor cell differentiation and function. *Trends Immunol.* 32:19–25. https://doi.org/10.1016/j.it.2010.10.002

Corzo, C.A., M.J. Cotter, P. Cheng, F. Cheng, S. Kusmartsev, E. Sotomayor, T. Padhya, T.V. McCaffrey, J.C. McCaffrey, and D.I. Gabrilovich. 2009. Mechanism regulating reactive oxygen species in tumor-induced myeloid-derived suppressor cells. *J. Immunol.* 182:5693–5701. https://doi.org/10.4049/jimmunol.0900092

Cui, Y.Z., H. Hisha, G.X. Yang, T.X. Fan, T. Jin, Q. Li, Z. Lian, and S. Ikehara. 2002. Optimal protocol for total body irradiation for allogeneic bone

marrow transplantation in mice. *Bone Marrow Transpl.* 30:843–849. https://doi.org/10.1038/sj.bmt.1703766

Daley, S.R., D.Y. Hu, and C.C. Goodnow. 2013. Helios marks strongly autoreactive CD4+ T cells in two major waves of thymic deletion distinguished by induction of PD-1 or NF-kappaB. *J. Exp. Med.* 210:269–285. https://doi.org/10.1084/jem.20121458

Dorhoi, A., and N. Du Plessis. 2017. Monocytic myeloid-derived suppressor cells in chronic infections. *Front. Immunol.* 8:1895. https://doi.org/10.3389/fimmu.2017.01895

European Association for the Study of the Liver. Electronic address: easloffice@easloffice.eu; 2017. EASL 2017 Clinical Practice Guidelines on the management of hepatitis B virus infection. *J. Hepatol.* 67:370–398. https://doi.org/10.1016/j.jhep.2017.03.021

Fang, Z., J. Li, X. Yu, D. Zhang, G. Ren, B. Shi, C. Wang, A.D. Kosinska, S. Wang, X. Zhou, M. Kozlowski, et al. 2015. Polarization of monocytic myeloid-derived suppressor cells by hepatitis B surface antigen is mediated via ERK/IL-6/STAT3 signaling feedback and restrains the activation of T cells in chronic hepatitis B virus infection. *J. Immunol.* 195:4873–4883. https://doi.org/10.4049/jimmunol.1501362

Gehring, A.J., M. Haniffa, P.T. Kennedy, Z.Z. Ho, C. Boni, A. Shin, N. Banu, A. Chia, S.G. Lim, C. Ferrari, F. Ginhoux, et al. 2013. Mobilizing monocytes to cross-present circulating viral antigen in chronic infection. *J. Clin. Invest.* 123:3766–3776. https://doi.org/10.1172/JCI66043

Hadeiba, H., K. Lahl, A. Edalati, C. Oderup, A. Habtezion, R. Pachynski, L. Nguyen, A. Ghodsi, S. Adler, and E.C. Butcher. 2012. Plasmacytoid dendritic cells transport peripheral antigens to the thymus to promote central tolerance. *Immunity.* 36:438–450. https://doi.org/10.1016/j.immuni.2012.01.017

Hakim, F.T., and R.E. Gress. 2007. Thymic involution: implications for self-tolerance. *Methods Mol. Biol.* 380:377–390. https://doi.org/10.1007/978-1-59745-395-0_24

He, Y.M., X. Li, M. Perego, Y. Nefedova, A.V. Kossenkov, E.A. Jensen, V. Kagan, Y.F. Liu, S.Y. Fu, Q.J. Ye, Y.H. Zhou, et al. 2018. Transitory presence of myeloid-derived suppressor cells in neonates is critical for control of inflammation. *Nat. Med.* 24:224–231. https://doi.org/10.1038/nm.4467

Hong, M., and A. Bertoletti. 2017. Tolerance and immunity to pathogens in early life: insights from HBV infection. *Semin. Immunopathol.* 39:643–652. https://doi.org/10.1007/s00281-017-0641-1

Hoogeveen, R.C., M.P. Robidoux, T. Schwarz, L. Heydmann, J.A. Cheney, D. Kvistad, J. Aneja, J.G. Melgaco, C.A. Fernandes, R.T. Chung, A. Boonstra, et al. 2019. Phenotype and function of HBV-specific T cells is determined by the targeted epitope in addition to the stage of infection. *Gut.* 68:893–904. https://doi.org/10.1136/gutjnl-2018-316644

Izhak, L., G. Wildbaum, U. Weinberg, Y. Shaked, J. Alami, D. Dumont, A. Stein, and N. Karin. 2010. Predominant expression of CCL2 at the tumor site of prostate cancer patients directs a selective loss of immunological tolerance to CCL2 that could be amplified in a beneficial manner. *J. Immunol.* 184:1092–1101. https://doi.org/10.4049/jimmunol.0902725

Kim, Y.S., M.J. Morgan, S. Choksi, and Z.G. Liu. 2007. TNF-induced activation of the Nox1 NADPH oxidase and its role in the induction of necrotic cell death. *Mol. Cell.* 26:675–687. https://doi.org/10.1016/j.molcel.2007.04.021

Koble, C., and B. Kyewski. 2009. The thymic medulla: a unique microenvironment for intercellular self-antigen transfer. *J. Exp. Med.* 206:1505–1513. https://doi.org/10.1084/jem.20082449

Kurtulus, S., P. Tripathi, M.E. Moreno-Fernandez, A. Sholl, J.D. Katz, H.L. Grimes, and D.A. Hildeman. 2011. Bcl-2 allows effector and memory CD8+ T cells to tolerate higher expression of Bim. *J. Immunol.* 186:5729–5737. https://doi.org/10.4049/jimmunol.1100102

Kusmartsev, S., Y. Nefedova, D. Yoder, and D.I. Gabrilovich. 2004. Antigen-specific inhibition of CD8+ T cell response by immature myeloid cells in cancer is mediated by reactive oxygen species. *J. Immunol.* 172:989–999. https://doi.org/10.4049/jimmunol.172.2.989

Lancaster, J.N., H.M. Thyagarajan, J. Srinivasan, Y. Li, Z. Hu, and L.I.R. Ehrlich. 2019. Live-cell imaging reveals the relative contributions of antigen-presenting cell subsets to thymic central tolerance. *Nat. Commun.* 10:2220. https://doi.org/10.1038/s41467-019-09727-4

Le Bert, N., U.S. Gill, M. Hong, K. Kunasegaran, D.Z.M. Tan, R. Ahmad, Y. Cheng, C.A. Dutertre, A. Heinecke, L. Rivino, A. Tan, et al. 2020. Effects of hepatitis B surface antigen on virus-specific and global T cells in patients with chronic HBV infection. *Gastroenterology* 159:652–664. https://doi.org/10.1053/j.gastro.2020.04.019

Lechner, M.G., D.J. Liebertz, and A.L. Epstein. 2010. Characterization of cytokine-induced myeloid-derived suppressor cells from normal human peripheral blood mononuclear cells. *J. Immunol.* 185:2273–2284. https://doi.org/10.4049/jimmunol.1000901

Lechner, M.G., C. Megiel, S.M. Russell, B. Bingham, N. Arger, T. Woo, and A.L. Epstein. 2011. Functional characterization of human Cd33+ and Cd11b+ myeloid-derived suppressor cell subsets induced from peripheral blood mononuclear cells co-cultured with a diverse set of human tumor cell lines. *J. Transl. Med.* 9:90. https://doi.org/10.1186/1479-5876-9-90

Li, X., Y. Xu, Y. Dong, X. Yang, B. Ye, Y. Wang, and Y. Chen. 2018. Monitoring the efficacy of infant hepatitis B vaccination and revaccination in 0- to 8-year-old children: protective anti-HBs levels and cellular immune responses. *Vaccine.* 36:2442–2449. https://doi.org/10.1016/j.vaccine.2018.03.044

Liaw, Y.F., and C.M. Chu. 2009. Hepatitis B virus infection. *Lancet.* 373:582–592. https://doi.org/10.1016/S0140-6736(09)60207-5

Lopes, N., A. Serge, P. Ferrier, and M. Irla. 2015. Thymic crosstalk coordinates medulla organization and T-cell tolerance induction. *Front. Immunol.* 6:365. https://doi.org/10.3389/fimmu.2015.00365

Ma, F., S. Li, X. Gao, J. Zhou, X. Zhu, D. Wang, Y. Cai, F. Li, Q. Yang, X. Gu, W. Ge, et al. 2019. Interleukin-6-mediated CCR9(+) interleukin-17-producing regulatory T cells polarization increases the severity of necrotizing enterocolitis. *EBioMedicine.* 44:71–85. https://doi.org/10.1016/j.ebiom.2019.05.042

Matsumura, S., K. Yamamoto, N. Shimada, N. Okano, R. Okamoto, T. Suzuki, T. Hakoda, M. Mizuno, T. Higashi, and T. Tsuji. 2001. High frequency of circulating HBcAg-specific CD8 T cells in hepatitis B infection: a flow cytometric analysis. *Clin. Exp. Immunol.* 124:435–444. https://doi.org/10.1046/j.1365-2249.2001.01561.x

Nagaraj, S., K. Gupta, V. Pisarev, L. Kinarsky, S. Sherman, L. Kang, D.L. Herber, J. Schneck, and D.I. Gabrilovich. 2007. Altered recognition of antigen is a mechanism of CD8+ T cell tolerance in cancer. *Nat. Med.* 13:828–835. https://doi.org/10.1038/nm1609

Nagaraj, S., A.G. Schrum, H.I. Cho, E. Celis, and D.I. Gabrilovich. 2010. Mechanism of T cell tolerance induced by myeloid-derived suppressor cells. *J. Immunol.* 184:3106–3116. https://doi.org/10.4049/jimmunol.0902661

Nitschke, K., H. Luxenburger, M.M. Kiraithe, R. Thimme, and C. Neumann-Haefelin. 2016. CD8+ T-cell responses in hepatitis B and C: the (HLA–) A, B, and C of hepatitis B and C. *Dig. Dis.* 34:396–409. https://doi.org/10.1159/000444555

Nunes-Alves, C., C. Nobrega, S.M. Behar, and M. Correia-Neves. 2013. Tolerance has its limits: how the thymus copes with infection. *Trends Immunol.* 34:502–510. https://doi.org/10.1016/j.it.2013.06.004

Ott, J.J., G.A. Stevens, J. Groeger, and S.T. Wiersma. 2012. Global epidemiology of hepatitis B virus infection: new estimates of age-specific HBsAg seroprevalence and endemicity. *Vaccine.* 30:2212–2219. https://doi.org/10.1016/j.vaccine.2011.12.116

Peranzoni, E., S. Zilio, I. Marigo, L. Dolcetti, P. Zanovello, S. Mandruzzato, and V. Bronte. 2010. Myeloid-derived suppressor cell heterogeneity and subset definition. *Curr. Opin. Immunol.* 22:238–244. https://doi.org/10.1016/j.coi.2010.01.021

Rivera-Nieves, J., J. Ho, G. Bamias, N. Ivashkina, K. Ley, M. Oppermann, and F. Cominelli. 2006. Antibody blockade of CCL25/CCR9 ameliorates early but not late chronic murine ileitis. *Gastroenterology.* 131:1518–1529. https://doi.org/10.1053/j.gastro.2006.08.031

Rivino, L., N. Le Bert, U.S. Gill, K. Kunasegaran, Y. Cheng, D.Z. Tan, E. Becht, N.K. Hansi, G.R. Foster, T.H. Su, T.C. Tseng, et al. 2018. Hepatitis B virus-specific T cells associate with viral control upon nucleos(t)ide-analogue therapy discontinuation. *J. Clin. Invest.* 128:668–681. https://doi.org/10.1172/JCI92812

Rolin, J., H. Vego, and A.A. Maghazachi. 2014. Oxidized lipids and lysophosphatidylcholine induce the chemotaxis, up-regulate the expression of CCR9 and CXCR4 and abrogate the release of IL-6 in human monocytes. *Toxins (Basel).* 6:2840–2856. https://doi.org/10.3390/toxins6092840

Sastry, K.S.R., C.T. Too, K. Kaur, A.J. Gehring, L. Low, A. Javiad, T. Pollicino, L. Li, P.T.F. Kennedy, U. Lopatin, P.A. Macary, et al. 2011. Targeting hepatitis B virus-infected cells with a T-cell receptor-like antibody. *J. Virol.* 85:1935–1942. https://doi.org/10.1128/JVI.01990-10

Schuch, A., E. Salimi Alizei, K. Heim, D. Wieland, M.M. Kiraithe, J. Kemming, S. Llewellyn-Lacey, O. Sogukpinar, Y. Ni, S. Urban, P. Zimmermann, et al. 2019. Phenotypic and functional differences of HBV core-specific versus HBV polymerase-specific CD8+ T cells in chronically HBV-infected patients with low viral load. *Gut.* 68:905–915. https://doi.org/10.1136/gutjnl-2018-316641

Shen, Z., H. Yang, S. Yang, W. Wang, X. Cui, X. Zhou, W. Liu, S. Pan, Y. Liu, J. Zhang, J. Zhang, et al. 2017. Hepatitis B virus persistence in mice reveals IL-21 and IL-33 as regulators of viral clearance. *Nat. Commun.* 8:2119. https://doi.org/10.1038/s41467-017-02304-7

Solito, S., V. Bronte, and S. Mandruzzato. 2011. Antigen specificity of immune suppression by myeloid-derived suppressor cells. *J. Leukoc. Biol.* 90: 31–36. https://doi.org/10.1189/jlb.0111021

Tan, M.C.B., P.S. Goedegebuure, B.A. Belt, B. Flaherty, N. Sankpal, W.E. Gillanders, T.J. Eberlein, C.S. Hsieh, and D.C. Linehan. 2009. Disruption of CCR5-dependent homing of regulatory T cells inhibits tumor growth in a murine model of pancreatic cancer. *J. Immunol.* 182:1746–1755. https://doi.org/10.4049/jimmunol.182.3.1746

Thapa, P., and D.L. Farber. 2019. The role of the thymus in the immune response. *Thorac. Surg. Clin.* 29:123–131. https://doi.org/10.1016/j.thorsurg.2018.12.001

Thimme, R., S. Wieland, C. Steiger, J. Ghrayeb, K.A. Reimann, R.H. Purcell, and F.V. Chisari. 2003. CD8(+) T cells mediate viral clearance and disease pathogenesis during acute hepatitis B virus infection. *J. Virol.* 77: 68–76. https://doi.org/10.1128/jvi.77.1.68-76.2003

Tian, Y., C.F. Kuo, O. Akbari, and J.H.J. Ou. 2016. Maternal-derived Hepatitis B virus e antigen alters macrophage function in offspring to drive viral persistence after vertical transmission. *Immunity*. 44:1204–1214. https://doi.org/10.1016/j.immuni.2016.04.008

Trivedi, P.J., T. Bruns, S. Ward, M. Mai, C. Schmidt, G.M. Hirschfield, C.J. Weston, and D.H. Adams. 2016. Intestinal CCL25 expression is increased in colitis and correlates with inflammatory activity. *J. Autoimmun.* 68:98–104. https://doi.org/10.1016/j.jaut.2016.01.001

Veis, D.J., C.L. Sentman, E.A. Bach, and S.J. Korsmeyer. 1993. Expression of the Bcl-2 protein in murine and human thymocytes and in peripheral T lymphocytes. *J. Immunol.* 151:2546–2554

Vicari, A.P., D.J. Figueroa, J.A. Hedrick, J.S. Foster, K.P. Singh, S. Menon, N.G. Copeland, D.J. Gilbert, N.A. Jenkins, K.B. Bacon, and A. Zlotnik. 1997. TECK: a novel CC chemokine specifically expressed by thymic dendritic cells and potentially involved in T cell development. *Immunity*. 7: 291–301. https://doi.org/10.1016/s1074-7613(00)80531-2

Wang, N., X. Qin, Y. Cao, B. Liang, K. Yu, and H. Ye. 2018. Plasma vascular non-inflammatory molecule 3 is associated with gastrointestinal acute graft-versus-host disease in mice. *J. Inflamm. (Lond).* 15:1. https://doi.org/10.1186/s12950-017-0178-z

Wang, Q., J. Zhou, B. Zhang, Z. Tian, J. Tang, Y. Zheng, Z. Huang, Y. Tian, Z. Jia, Y. Tang, J.C. van Velkinburgh, et al. 2013. Hepatitis B virus induces IL-23 production in antigen presenting cells and causes liver damage via the IL-23/IL-17 axis. *PLoS Pathog.* 9:e1003410. https://doi.org/10.1371/journal.ppat.1003410

Yamano, T., J. Nedjic, M. Hinterberger, M. Steinert, S. Koser, S. Pinto, N. Gerdes, E. Lutgens, N. Ishimaru, M. Busslinger, B. Brors, et al. 2015. Thymic B cells are licensed to present self antigens for central T cell tolerance induction. *Immunity*. 42:1048–1061. https://doi.org/10.1016/j.immuni.2015.05.013

Yang, F., X. Yu, C. Zhou, R. Mao, M. Zhu, H. Zhu, Z. Ma, B. Mitra, G. Zhao, Y. Huang, H. Guo, et al. 2019. Hepatitis B e antigen induces the expansion of monocytic myeloid-derived suppressor cells to dampen T-cell function in chronic hepatitis B virus infection. *PLoS Pathog.* 15:e1007690. https://doi.org/10.1371/journal.ppat.1007690

Yang, P.L., A. Althage, J. Chung, and F.V. Chisari. 2002. Hydrodynamic injection of viral DNA: a mouse model of acute hepatitis B virus infection. *Proc. Natl. Acad. Sci. USA.* 99:13825–13830. https://doi.org/10.1073/pnas.202398599

Ye, P., and D.E. Kirschner. 2002. Reevaluation of T cell receptor excision circles as a measure of human recent thymic emigrants. *J. Immunol.* 168: 4968–4979. https://doi.org/10.4049/jimmunol.168.10.4968

Zanetti, F., M. Giacomello, Y. Donati, S. Carnesecchi, M. Frieden, and C. Barazzone-Argiroffo. 2014. Nicotine mediates oxidative stress and apoptosis through cross talk between NOX1 and Bcl-2 in lung epithelial cells. *Free Radic. Biol. Med.* 76:173–184. https://doi.org/10.1016/j.freeradbiomed.2014.08.002

Zehner, M., and S. Burgdorf. 2013. Regulation of antigen transport into the cytosol for cross-presentation by ubiquitination of the mannose receptor. *Mol. Immunol.* 55:146–148. https://doi.org/10.1016/j.molimm.2012.10.010

Supplemental material

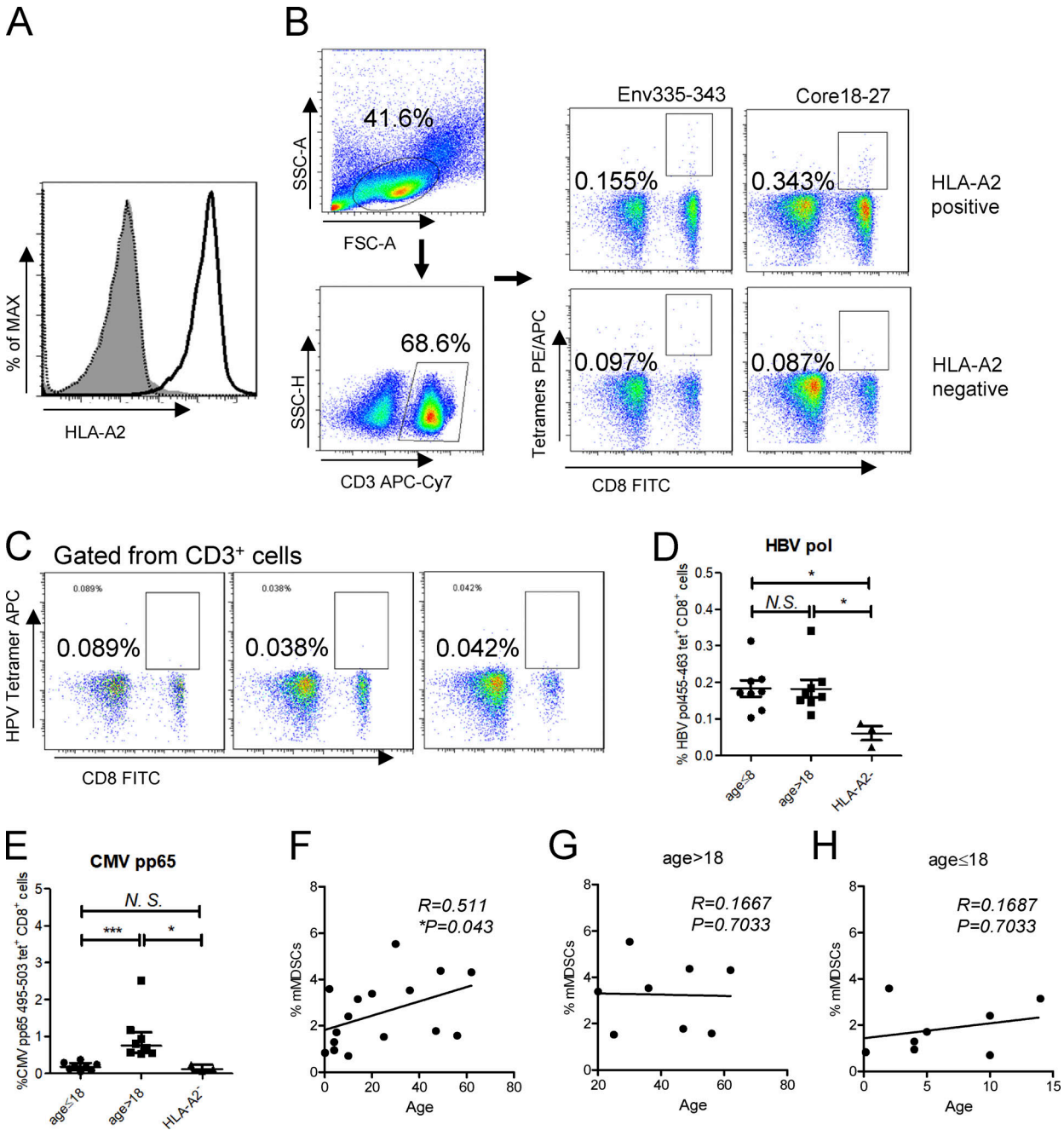

Figure S1. **Analysis of HBV-specific CD8⁺ cells in PBMCs from CHB patients. (A)** Detecting HLA-A2 expression on PBMCs from CHB patients. **(B)** Gating strategy of flow cytometry for HBsAg-specific (Env335-343) and HBcAg-specific (Core18-27) CD8⁺ T cells from PBMCs. **(C)** Analysis of HPV-specific CD8⁺ cells from three HLA-A2–positive CHB patients. **(D and E)** Comparing the frequencies of HBV polymerase–specific (D) or CMV pp65–specific (E) CD8⁺ T cells between subjects at different ages. **(F)** Correlating age with the frequency of mMDSCs in in CHB patients (n = 40). **(G and H)** Correlated age with the frequency of mMDSCs in in CHB patients at age > 18 (n = 20; G) or at age ≤ 18 (n = 20; H). *, P < 0.05; ***, P < 0.001.

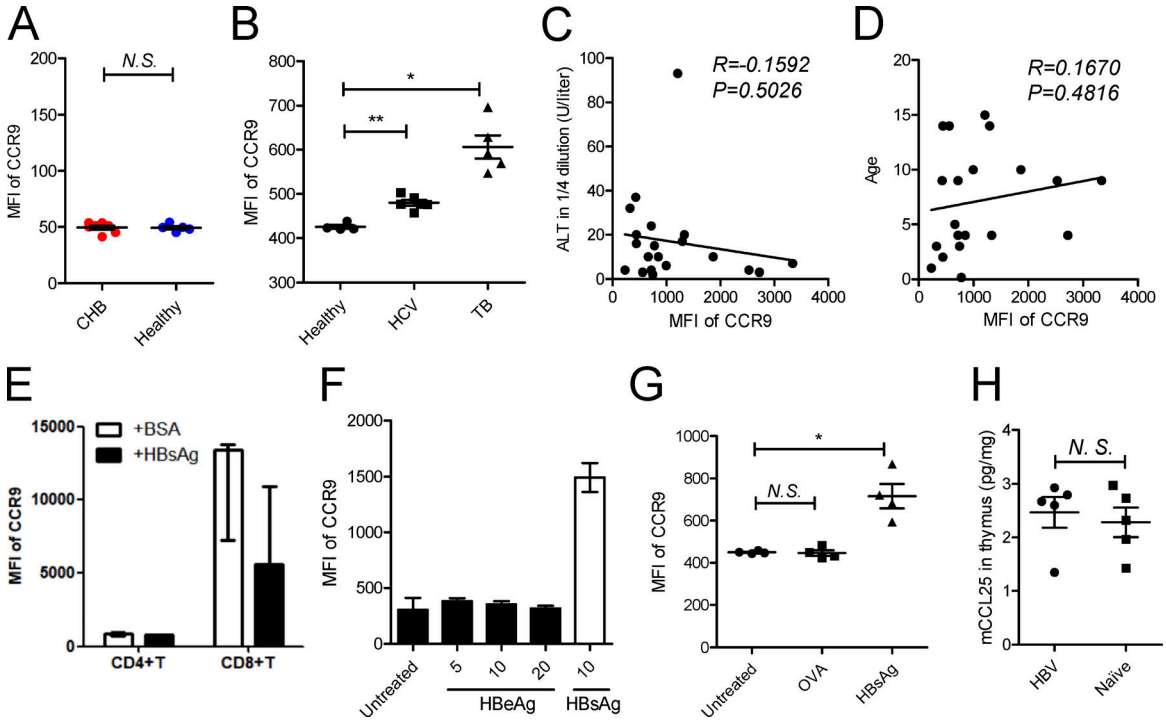

Figure S2. **Analyzing the expression of chemokine receptors on mMDSCs. (A)** Level of CCR9 on total CD14⁻ cells in CHB patients (n = 7) and healthy donors (n = 5). **(B)** Level of CCR9 on CD14⁺ myeloid cells in blood from chronic HCV and TB infection. **(C and D)** Correlation between serum ALT (C) or age (D) with median fluorescence intensity (MFI) of CCR9 on mMDSCs from CHB patients (age < 20, n = 20). **(E)** Detection of CCR9 on CD4⁺ or CD8⁺ T cells after stimulating healthy PBMCs with HBsAg (n = 3). **(F)** Detecting CCR9 on mMDSCs after stimulation with HBeAg in different concentrations or HBsAg (μg/ml). **(G)** Detecting CCR9 after stimulation with OVA or HBsAg. **(H)** Detection of CCL25 in the thymus from HBV-persistent HDI mice or naive mice (n = 5). *, P < 0.05; **, P < 0.01.

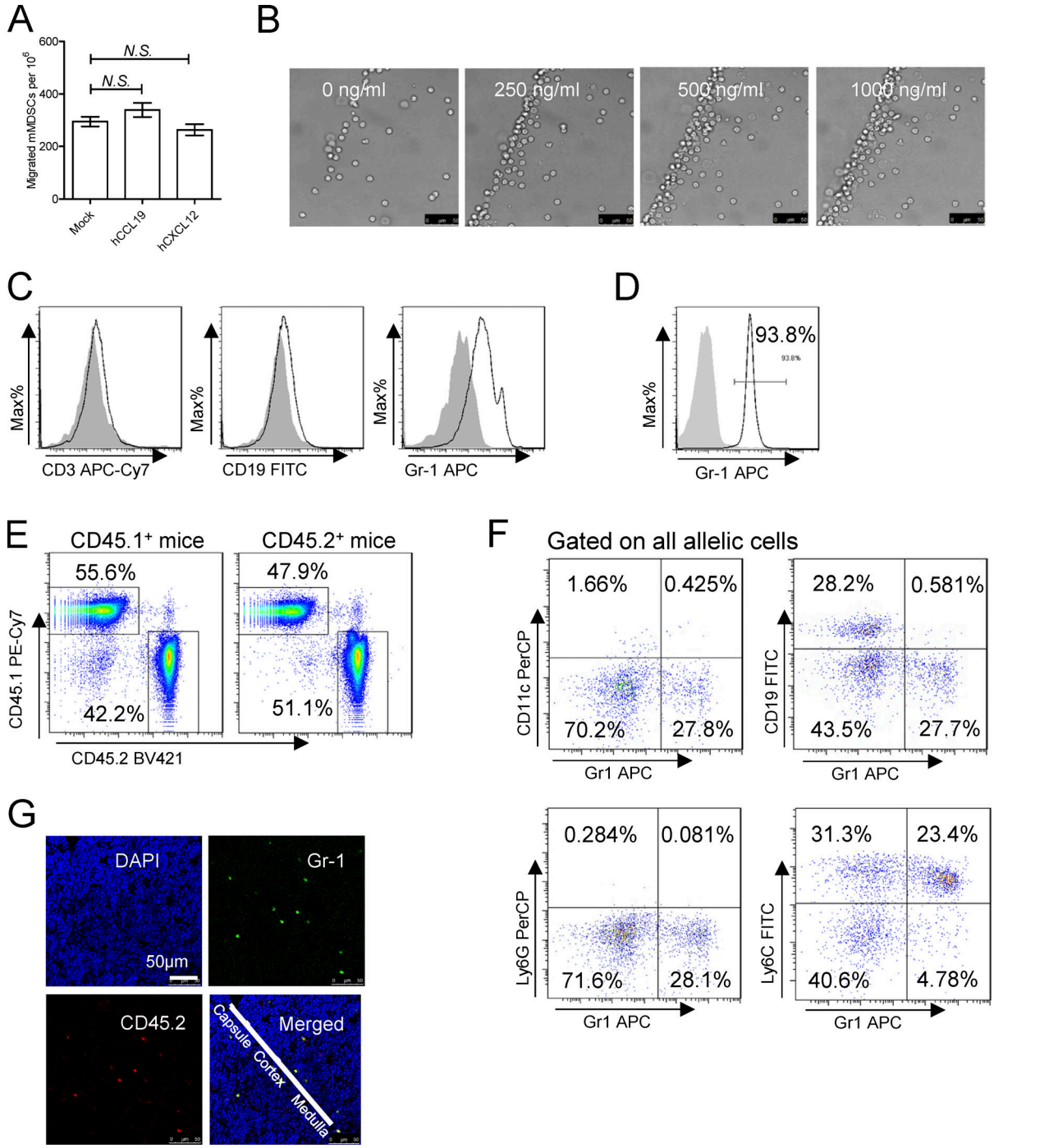

Figure S3. **Migration of mMDSCs. (A)** Transwell migration study of mMDSCs from CHB patients toward hCCL19 or hCXCL12 (n = 3, 500 ng/ml). **(B)** Dose-dependent migration of purified mouse mMDSCs toward agarose dots containing mCCL25, triplicate. Scale bars, 50 μm. **(C)** Identifying surface markers (CD3, CD19, and Gr-1) on migrated cells from the Transwell study. **(D)** Purity of mMDSCs using for adoptive transfer (ADT). **(E)** Detection of allelic cells in the blood from surgically joined CD45.2$^+$ and CD45.1$^+$ mice. **(F)** Flow cytometry analyzing the expression of CD11c, CD19, Ly6G, and Ly6C on allelic mMDSCs from the parabiosis study. **(G)** Detection of allelic mMDSCs in the thymus of CD45.1$^+$ mice transferred with CD45.2$^+$ mMDSCs from HBV-persistent HDI mice, IF, triplicate.

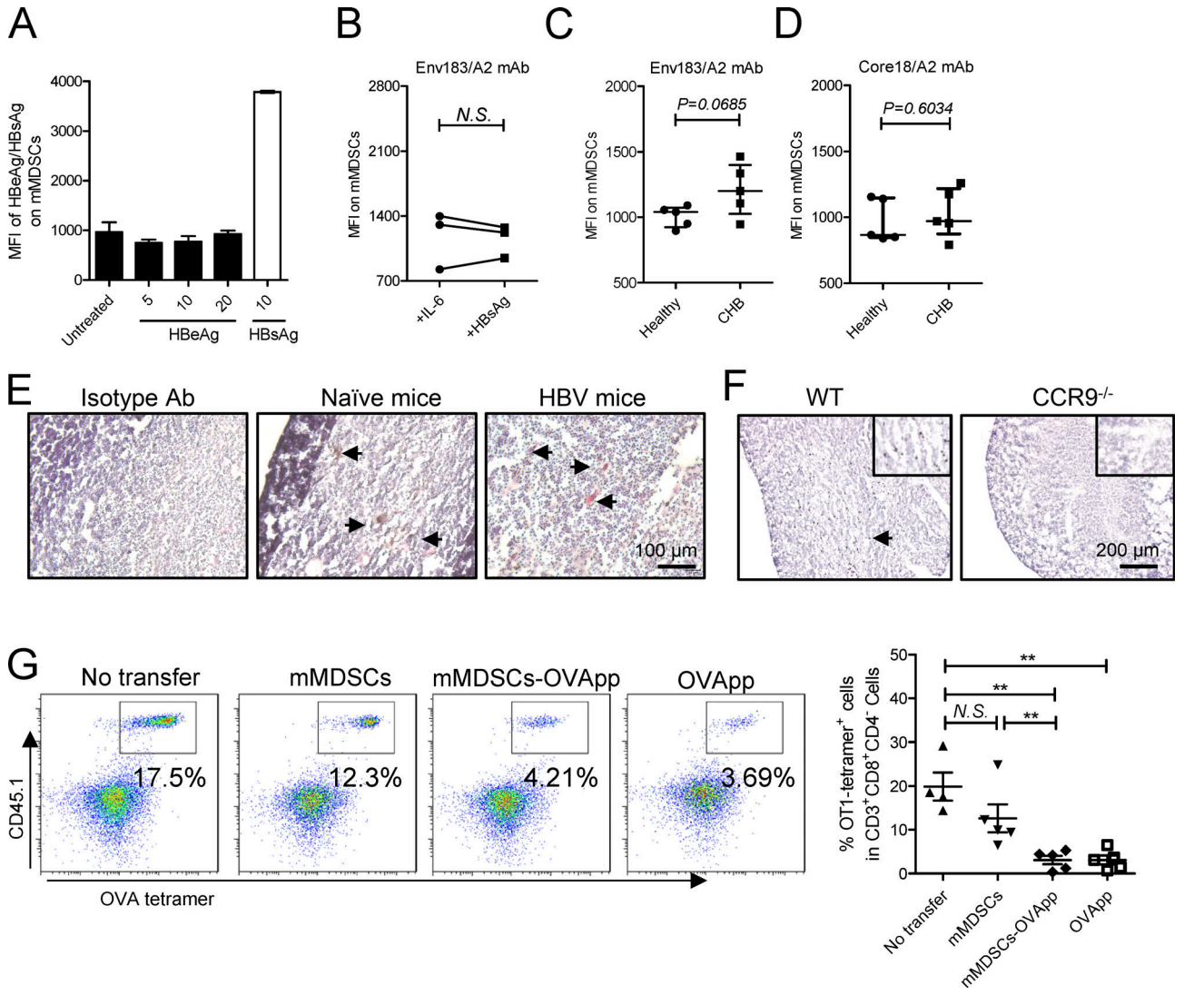

Figure S4. **Antigen transfer and thymocyte deletion by mMDSCs. (A)** Detection of HBeAg or HBsAg in their stimulated mMDSCs (μg/ml). **(B)** Detection of the Env183/A2 complex on IL-6 or HBsAg-induced HLA-A2–negative mMDSCs with TCR-like antibody (n = 7). **(C)** Flow cytometry determining MFI of the Env183/A2 complex on HLA-A2–positive mMDSCs from CHB and CD14$^+$ myeloid cells from healthy donors. **(D)** Flow cytometry determining MFI of the Core18/A2 complex on HLA-A2–positive mMDSCs from CHB and CD14$^+$ myeloid cells from healthy donors. **(E)** IHC staining of HBsAg in the thymus from HBV-persistent HDI mice. Nucleus (violet), Gr-1 (brown), HBsAg (red), IHC, 200X, triplicate. Arrows indicate the positive signaling in the IHC staining. **(F)** Detection of HBsAg in the thymus from WT and CCR9$^{-/-}$ HBV-persistent HDI mice (brown, 100X), triplicate. Arrows indicate the positive signaling in the IHC staining. **(G)** Detecting OVA-specific CD8$^+$ thymocytes via flow cytometry in reconstituted mice on day 3 after transfer of OVApp 257-264-loaded mMDSCs (10^7 cells per mice, n = 5). **, P < 0.01.

Provided online is Table S1. Table S1 shows the characteristics of CHB patients.